

Iowa State University

---

From the Selected Works of Yan Zhao

---

April, 1996

## $\beta$ Effect of Phosphorus Functionalities

Joseph B. Lambert, *Northwestern University*

Yan Zhao, *Northwestern University*



Available at: [https://works.bepress.com/yan\\_zhao/47/](https://works.bepress.com/yan_zhao/47/)

## $\beta$ Effect of Phosphorus Functionalities

Joseph B. Lambert\* and Yan Zhao

Contribution from the Department of Chemistry, Northwestern University, Evanston, Illinois 60208-3113

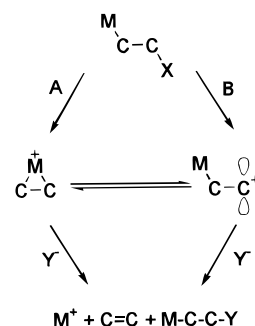
Received November 3, 1995<sup>⊗</sup>

**Abstract:** Diphenylphosphinoyl ( $-\text{P}(=\text{O})\text{Ph}_2$ ) and diphenylthiophosphinoyl ( $-\text{P}(=\text{S})\text{Ph}_2$ ) respectively are modest and strong  $\beta$ -effect functionalities. When these groups are antiperiplanar to mesylate, the substrates solvolyze through unimolecular ionization. In contrast, substrates with the synclinal (*gauche*) arrangement react bimolecularly with solvent. The anti/*gauche* rate ratio is 440 for the oxide and  $3.2 \times 10^6$  for the sulfide at 25 °C. The antiperiplanar sulfide in fact reacts 220 times more rapidly than the analogous cyclohexyl substrate at 25 °C, despite the strong electron-withdrawing nature of diphenylthiophosphinoyl. The  $\alpha$ -secondary hydrogen/deuterium kinetic isotope effects of 1.21 for the anti oxide and 1.26 for the anti sulfide suggest high  $\text{sp}^2$  character in the transition state, as expected for stabilization by hyperconjugation in a vertical mechanism. Energies calculated at the MP2 level show that the geometry with the P–C bond parallel to the empty carbocation p orbital is more stable than the perpendicular geometry by 22.94 kcal mol<sup>-1</sup> for  $\text{PH}_2$ , 8.80 kcal mol<sup>-1</sup> for  $\text{P}(\text{O})\text{H}_2$ , and 10.54 kcal mol<sup>-1</sup> for  $\text{P}(\text{S})\text{H}_2$ , confirming significant hyperconjugation for these substituents. The global minimum, however, is the bridged structure (four-membered rings for the oxide and sulfide, three-membered ring for the simple phosphine), so that the mechanistic choice between a vertical mechanism (hyperconjugation) and a nonvertical mechanism (bridging) is not clear-cut.

The formation of positive charge on carbon by cleavage of a C–X bond may be accelerated by the presence of certain atoms or groups (M) attached to the adjacent or  $\beta$  carbon (M–C–C–X). Two mechanisms of interaction between M and the developing positive charge on carbon have been considered (Scheme 1). In path A the group M attacks the backside of the C–X bond in an intramolecular displacement to form a ring. This mode has variously been called internal displacement, anchimeric assistance, neighboring group participation, bridging, or nonvertical participation. A wide variety of M groups have been implicated in this mode of reactivity, including halogens, amines, sulfides, alkoxy/alkoxides (all forming three-membered rings), and acetoxy (forming a five-membered ring). This field is part of classic mechanistic organic chemistry.<sup>1</sup> The nucleophilic entity on all these functionalities is a lone pair of electrons (the analogous reactions of  $\pi$  electrons are not under consideration here).

The examination of strong electron donors such as silicon that lack lone pairs or  $\pi$  electrons led to serious consideration of path B in Scheme 1, which has variously been called hyperconjugation, vertical participation, nonbridging, open, or  $\sigma\pi$  conjugation.<sup>2</sup> A highly polarizable and electron rich M–C bond can stabilize the developing positive charge with minimal alteration of the geometry around the M–C bond. In contrast to path A, the transition state for path B has strong  $\text{sp}^2$  character for the carbon bearing positive charge, and the open carbocation can lead to a range of elimination and rearranged substitution products. Silicon was the first such  $\beta$ -effect heteroatom to be studied extensively<sup>2</sup> followed by germanium, tin, lead,<sup>3</sup> and mercury.<sup>3,4</sup>

Scheme 1



The most effective criteria for distinguishing between these two modes of involvement have been stereochemistry,<sup>2,5</sup> kinetic isotope effect,<sup>6</sup> and product studies. The optimum geometry for nonvertical participation (path A) is the antiperiplanar arrangement of the M–C–C–X fragment. All other geometries are ineffective, as the displacement must occur on the backside. Hyperconjugation in the transition state for path B, however, is modulated as the cosine-squared function of the M–C–C–X dihedral angle, with favorable interactions occurring at both the antiperiplanar (180°) and synperiplanar (0°) geometries.<sup>5</sup> Path A should have an  $\alpha$ -secondary kinetic deuterium isotope effect ( $k_{\text{H}}/k_{\text{D}}$  for H and D on the carbon attached to the leaving group X) of 1.00–1.05, since the transition state resembles a trigonal bipyramid. For path B the transition state has  $\text{sp}^2$  character at this carbon, with the expectation of an isotope effect close to 1.20.<sup>6</sup> The substitution products (M–C–C–Y if the nucleophile is  $\text{Y}^-$  or HY) are expected to be formed with retention of configuration at carbon as the result of two consecutive inversions in the bridging mechanism of path A. Carbocationic intermediates in path B should not exhibit retention in substitution products.

Finally, two subtleties of these mechanisms should be noted. The bridged and open carbocation intermediates may be in

<sup>⊗</sup> Abstract published in *Advance ACS Abstracts*, March 15, 1996.

(1) Gould, E. S. *Mechanism and Structure in Organic Chemistry*; Holt, Rinehart and Winston: New York, 1959; Chapter 14.

(2) For the case of the  $\beta$  effect of silicon, see: Lambert, J. B. *Tetrahedron* **1990**, *46*, 2677–2689 and references therein.

(3) Davis, D. D.; Gray, C. E. *J. Org. Chem.* **1970**, *35*, 1303–1307. Jerkunica, J. M.; Traylor, T. G. *J. Am. Chem. Soc.* **1971**, *93*, 6278–6279. Lambert, J. B.; Wang, G.-t.; Teramura, D. H. *J. Org. Chem.* **1988**, *53*, 5422–5428.

(4) Kreevoy, M. M.; Kowitz, F. R. *J. Am. Chem. Soc.* **1960**, *82*, 739–745. Lambert, J. B.; Emblidge, R. W. *J. Phys. Org. Chem.* **1993**, *6*, 555–560.

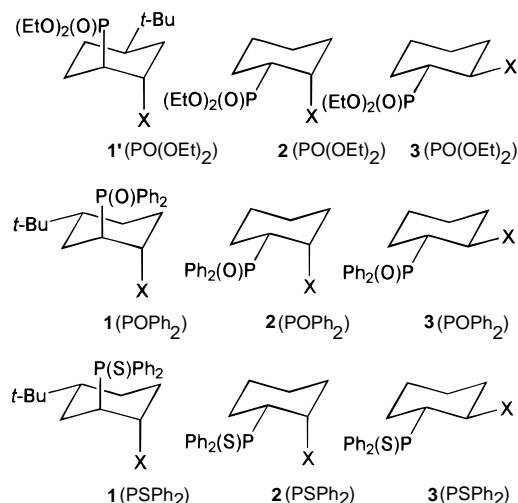
(5) Lambert, J. B.; Chelius, E. C. *J. Am. Chem. Soc.* **1990**, *112*, 8120–8126.

(6) Lambert, J. B.; Emblidge, R. W.; Malany, S. *J. Am. Chem. Soc.* **1993**, *115*, 1317–1320.

equilibrium, as noted in Scheme 1. Thus the rate-determining step may lead to one intermediate, which equilibrates with the other form, and products may be formed from either structure. Secondly, there may be strong vertical stabilization of the open carbocation, but the nonvertical pathway can still be kinetically favored.

Few if any phosphorus functionalities have been examined as potential  $\beta$ -effect groups. Phosphines with the requisite saturated group ( $R_2P-CH_2CH_2X$ ) tend to be highly air and water sensitive and probably have not been examined, primarily because they are difficult to handle. In more stable higher valencies, in which the lone pair is replaced by a heteroatom such as oxygen or sulfur, the phosphorus functionality is extremely electron withdrawing, making the cationic reactions of Scheme 1 very slow. The ability of  $\alpha$ -electron-withdrawing groups to stabilize cations has been the subject of considerable recent investigation.<sup>7</sup> The only  $\beta$ -electron-withdrawing group (by  $\sigma_p$ ) that has been studied is carbonyl.<sup>8ab</sup> Appreciable rate accelerations are observed only for  $\gamma$ - and  $\delta$ -carbonyl groups (ketones and esters), which form five- and six-membered rings via path A (including Winstein's famous acetoxonium ions). Little or no rate acceleration is observed for closure of four-membered rings by  $\beta$ -carbonyl groups (the oxygen is the nucleophile). Path A to form a four-membered ring thus is not expected to be a kinetically favorable mechanism, from the carbonyl precedents. Destabilization of an open carbocation by the polar effect of a strongly electron-withdrawing  $\beta$  group (M), however, also militates against path B. Electron-withdrawing groups on silicon usually shut down its  $\beta$  activity.<sup>8c</sup> Thus prior work with electron-withdrawing  $\beta$  groups was not encouraging.

We have recently evaluated diethyl phosphonate ( $P(O)(OEt)_2$ ) as a potential  $\beta$ -effect group.<sup>9</sup> Our approach was to compare the systems in which the  $M-C-C-X$  ( $M = P(O)(OEt)_2$ ,  $X = OTs$ ) fragment is part of a cyclohexane system. The geometry of the cyclohexane ring permits two stereochemistries, in which the  $M-C-C-X$  dihedral angles respectively are antiperiplanar in the biased trans form **1** or **1'** and synclinal in the cis form **2**.



For the phosphonate case, we prepared **1'**. In addition, we examined the unbiased trans form **3**, which is a conformational mix of the two stereochemistries. We found that the cis form

solvolyzes by solvent participation ( $k_s$ ), analogous to  $S_N2$  or  $E_2$ , but the biased trans form solvolyzes by a carbocation pathway ( $k_c$ ), analogous to  $S_N1$  or  $E_1$ , or by anchimeric assistance ( $k_A$ ). The rate acceleration of the biased trans form over the cis form was 12.7 in 97% trifluoroethanol (TFE) at 25 °C and 19.4 in hexafluoro-2-propanol (HFIP) at 70 °C. This modest acceleration means that the biased trans form solvolyzes more slowly than cyclohexyl tosylate, by a factor of about 15, a number that still is remarkably small for such a strongly electron-withdrawing group. This study showed that the anti-periplanar diethyl phosphonate group changes the mechanism from the normal  $k_s$  process for a cyclohexyl tosylate to a unimolecular ionization process and that the effect has a stereochemical dependence. Thus diethyl phosphonate joined carbonyl<sup>8</sup> as an electron-withdrawing group that exhibits weak  $\beta$ -effect activity.

This study left many questions unanswered. Although hyperconjugation (path B) could explain the results, the possibility that the phosphonate group could nucleophilically participate to form a four-membered ring (path A) was not eliminated.<sup>9</sup> Product studies provided the only evidence favoring hyperconjugation over bridging. Phosphonate in its most favorable stereochemistry (**1'**) did not provide a net rate acceleration with respect to cyclohexyl, so that it clearly was at best a weak  $\beta$ -effect group: strong enough to alter the mechanism to  $k_c$  or  $k_A$  but still too weak to provide a rate acceleration. In contrast, trimethylsilyl causes an acceleration<sup>2</sup> of at least  $10^{12}$ . Consequently, we have sought other potential phosphorus-containing  $\beta$ -effect groups and report herein our results with phosphine oxide and phosphine sulfide.

Our phosphonate work was inspired by the observation by Mastalerz et al. that the phosphonic acid group ( $P(O)(OH)_2$ ) undergoes a Wagner–Meerwein 1,2-shift intact.<sup>10</sup> The group must have some carbocation-stabilizing ability in order to retain P–C bonding (bridging would lead to P–O bonding). Warren et al. analogously observed that phosphine oxides undergo Wagner–Meerwein rearrangement intact.<sup>11</sup> Since phosphine oxide is encumbered with fewer electron-withdrawing oxygen atoms than phosphonate, we thought that it might be a better  $\beta$ -effect group. By further analogy, phosphine sulfides should have increased polarizability and provide even better hyperconjugation. We report herein the experimental studies that demonstrate that these functionalities are modest to strong  $\beta$ -effect groups. We have also examined  $P(O)(OH)_2$ ,  $P(O)H_2$ ,  $P(S)H_2$ , and  $PH_2$  computationally in the system  $M-CH_2-CHMe^+$  in order to assess their hyperconjugative and bridging abilities.

## Experimental Results and Discussion

**Synthesis.** The synthetic manipulations are summarized in Scheme 2. The unbiased trans phosphine oxide **3**( $POPh_2$ )-OH was prepared readily by ring opening of cyclohexene oxide with diphenylphosphide anion followed by oxidation with hydrogen peroxide. A mixture of *cis*- and *trans*-4-*tert*-butylcyclohexene oxide was treated in the same fashion to give the biased trans oxide **1**( $POPh_2$ )-OH after purification. Its structure was confirmed by 1D and 2D NMR experiments. The phosphinoyl group of the unbiased trans compound was equilibrated with butyllithium to a *cis*/*trans* mixture, from which the *cis* oxide **2**( $POPh_2$ )-OH was obtained by chromatography. For the  $\alpha$ -deuterated version of the biased trans oxide, **1**( $POPh_2-d$ )-OH, 4-*tert*-butylcyclohexanone was reduced to the alcohol with

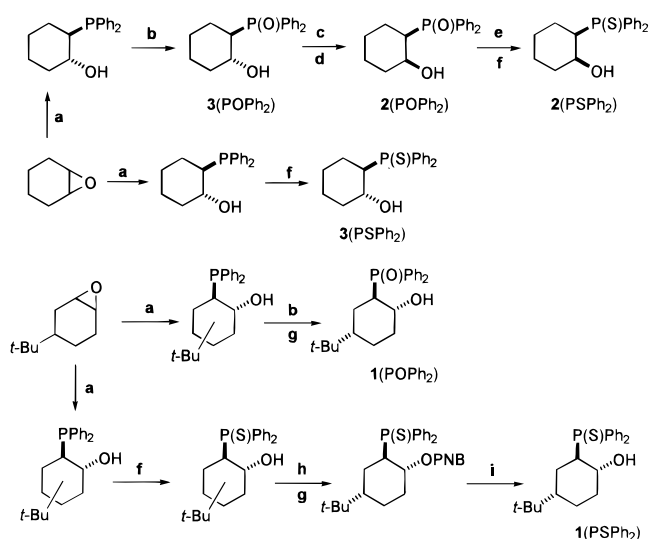
(7) Creary, X. *Chem. Rev.* **1991**, *91*, 1625–1678.

(8) (a) Yoshida, M.; Takeuchi, K. *J. Org. Chem.* **1993**, *58*, 2566–2572. (b) Perst, H. *Oxonium Ions in Organic Chemistry*; Verlag Chemie: Weinheim, Germany, 1971; Chapter 6. (c) In addition,  $\beta$  silicon has been made electron withdrawing by halogen substitution: Brook, M. A.; Neuy, A. *J. Org. Chem.* **1990**, *55*, 3609–3616.

(9) Lambert, J. B.; Emblidge, R. W.; Zhao, Y. *J. Org. Chem.* **1994**, *59*, 5397–5403.

(10) Richtarski, G.; Mastalerz, P. *Tetrahedron Lett.* **1973**, 4069–4070. Richtarski, G.; Soroka, M.; Mastalerz, P.; Starzemska, H. *Rocz. Chem. Ann. Soc. Chim. Pol.* **1975**, *49*, 2001–2005; *Chem. Abstr.* **1976**, *85*, 5576x.

(11) Cann, P. F.; Warren, S. J. *Chem. Soc., Chem. Commun.* **1970**, 1026–1027. Cann, P. F.; Howells, D.; Warren, S. J. *Chem. Soc., Perkin Trans. 2* **1972**, 304–311.

Scheme 2<sup>a</sup>

<sup>a</sup> (a)  $\text{Ph}_2\text{PLi}$ ; (b)  $\text{H}_2\text{O}_2$ ; (c)  $\text{BuLi}$ ; (d)  $\text{H}_3\text{O}^+$ , chromatography; (e)  $\text{HSiCl}_3/\text{pyridine}$ ; (f) sulfur; (g) crystallization; (h) *p*-nitrobenzoyl chloride/pyridine; (i)  $\text{K}_2\text{CO}_3/\text{MeOH}$ .

Table 1. Rate Constants for the Phosphine Oxides ( $M = \text{P}(\text{O})\text{Ph}_2$ )

substrate	solvent <sup>a</sup>	temp, °C	rate, s <sup>-1</sup>		
1-OMs (biased trans)	97% TFE	70.0	$5.37 \times 10^{-4}$		
		65.0	$3.12 \times 10^{-4}$		
		55.0	$9.95 \times 10^{-5}$		
		47.0	$3.79 \times 10^{-5}$		
		45.0 <sup>b</sup>	$2.95 \times 10^{-5}$		
	80% TFE	25.0 <sup>b</sup>	$2.05 \times 10^{-6}$		
		65.0	$3.86 \times 10^{-4}$		
		80% EtOH	65.0	$7.58 \times 10^{-5}$	
		70% EtOH	65.0	$1.33 \times 10^{-4}$	
		60% EtOH	65.0	$1.90 \times 10^{-4}$	
1-1- <i>d</i> -OMs (biased trans)	97% TFE	45.0	$5.74 \times 10^{-4}$		
		55.0	$8.17 \times 10^{-5}$		
2-OMs (cis)	97% TFE	95.0	$8.04 \times 10^{-6}$		
		90.0	$4.83 \times 10^{-6}$		
		85.0	$3.07 \times 10^{-6}$		
		80.0	$2.09 \times 10^{-6}$		
		70.0 <sup>b</sup>	$7.68 \times 10^{-7}$		
		25.0 <sup>b</sup>	$4.62 \times 10^{-9}$		
		75.0	$1.25 \times 10^{-4}$		
3-OMs (trans)	97% TFE	65.0	$3.69 \times 10^{-5}$		
		55.0	$1.11 \times 10^{-5}$		
		25.0 <sup>b</sup>	$1.58 \times 10^{-7}$		
		80% TFE	65.0	$4.88 \times 10^{-5}$	
		60% TFE	65.0	$6.48 \times 10^{-5}$	
	80% EtOH	65.0	$2.08 \times 10^{-5}$		
		70% EtOH	65.0	$2.74 \times 10^{-5}$	
		60% EtOH	65.0	$5.16 \times 10^{-5}$	
		cyclohexyl mesylate	97% TFE	70.0 <sup>c</sup>	$1.79 \times 10^{-4}$
				65.0 <sup>c</sup>	$1.21 \times 10^{-4}$
45.0 <sup>c</sup>	$2.22 \times 10^{-5}$				
25.0 <sup>c</sup>	$3.24 \times 10^{-6}$				
	97% HFIP	45.0	$1.69 \times 10^{-4}$		

<sup>a</sup> Percentages are wt/wt for trifluoroethanol (TFE) and hexafluoro-2-propanol (HFIP) and v/v for ethanol (EtOH). <sup>b</sup> Calculated from rates at other temperatures. <sup>c</sup> Calculated from ref 5.

lithium aluminum deuteride, the alcohol was converted to 4-*tert*-butylcyclohexene-1-*d* by treatment with mesyl chloride and collidine, the alkene was epoxidized, and the epoxide was ring opened to the desired product on purification.

The unbiased trans phosphine sulfide **3**(PSPH<sub>2</sub>)-OH was prepared in the same fashion but with treatment of the intermediate phosphine with elemental sulfur instead of hydrogen peroxide. An analogous procedure also produced the biased trans sulfide **1**(PSPH<sub>2</sub>)-OH, although the final isomeric mixture could not be separated. As a result, the method (locally

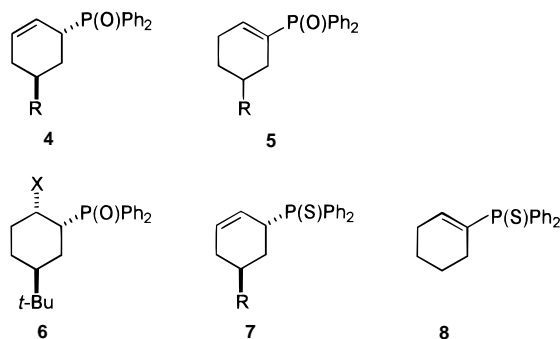
Table 2. Rate Constants for Phosphine Sulfides ( $M = \text{P}(\text{S})\text{Ph}_2$ )

substrate	solvent <sup>a</sup>	temp, °C	rate, s <sup>-1</sup>	
1-OMs (biased trans)	97% TFE	70.0 <sup>b</sup>	$9.34 \times 10^{-2}$	
		35.1	$2.45 \times 10^{-3}$	
		30.0	$1.32 \times 10^{-3}$	
		25.0	$7.27 \times 10^{-4}$	
		35.1	$1.95 \times 10^{-3}$	
1-1- <i>d</i> -OMs (biased trans)	97% TFE	95.0	$8.13 \times 10^{-6}$	
		90.0	$4.71 \times 10^{-6}$	
		85.0	$2.22 \times 10^{-6}$	
		80.0	$1.26 \times 10^{-6}$	
		70.0 <sup>b</sup>	$3.18 \times 10^{-7}$	
2-OMs (cis)	97% TFE	25.0 <sup>b</sup>	$2.28 \times 10^{-10}$	
		65.0	$8.49 \times 10^{-4}$	
		60.0	$4.86 \times 10^{-4}$	
		55.0	$2.54 \times 10^{-4}$	
		25.0 <sup>b</sup>	$4.22 \times 10^{-6}$	
	80% TFE	65.0	$6.78 \times 10^{-4}$	
		60% TFE	65.0	$6.03 \times 10^{-4}$
		80% EtOH	65.0	$8.49 \times 10^{-5}$
		70% EtOH	65.0	$1.29 \times 10^{-4}$
		60% EtOH	65.0	$1.49 \times 10^{-4}$

<sup>a</sup> See footnote a in Table 1. <sup>b</sup> Calculated from rates at other temperatures.

modified) of Rickborn and Quartucci<sup>12</sup> was used to obtain the pure product by conversion to the *p*-nitrobenzoate, recrystallization, and hydrolysis. The cis sulfide **2**(PSPH<sub>2</sub>)-OH was obtained from the analogous phosphine oxide by treatment with pyridine and trichlorosilane to form the phosphine followed by treatment with sulfur. The structures of the cis sulfide and the biased trans sulfide were determined by X-ray crystallography as *p*-nitrobenzoate derivatives, the details of which are given in the Experimental Section. The deuterated biased trans sulfide **1**(PSPH<sub>2</sub>-*d*)-OH was obtained from 4-*tert*-butylcyclohexene-1-*d* as with the undeuterated version.

**Kinetics.** The alcohols were converted to the mesylates and solvolyzed in aqueous mixtures of ethanol (EtOH), trifluoroethanol, and hexafluoro-2-propanol. The rates for the oxides are given in Table 1 and those for the sulfides in Table 2. Experiments were carried out as a function of temperature in 97% TFE, and the activation parameters are given in Table 3. Rober-Harris plots were carried out for the biased trans oxide (Figure 1), the unbiased trans oxide (Figure 2), and the unbiased trans sulfide (Figure 3). The rates of the cis oxide and sulfide were too slow to provide the ethanol data for such a plot, and the plot was deemed unnecessary for the biased trans sulfide. Product studies were carried out in both 97% TFE and 80% EtOH. The products include structures **4–8**, whose proportions are given in Table 4.



**Kinetic Comparisons.** Both anchimeric assistance and hyperconjugation should be manifested by a rate enhancement. We have made comparisons in two ways. First, the ratio of the functionalized systems **1–3** to cyclohexyl for the same leaving group X gives an overall measure of the effect of M,

**Table 3.** Activation Parameters in 97% TFE at 25 °C

substrate	$E_a$ , kcal mol <sup>-1</sup>	log A	$\Delta H^\ddagger$ , kcal mol <sup>-1</sup>	$\Delta S^\ddagger$ , cal deg <sup>-1</sup> mol <sup>-1</sup>	$\Delta G^\ddagger$ , kcal mol <sup>-1</sup>	$\rho^b$
<b>1</b> (POPh <sub>2</sub> )-OMs (biased trans)	25.2	12.76	24.5	-2.3	25.2	1.000
<b>2</b> (POPh <sub>2</sub> )-OMs (cis)	23.2	8.65	22.5	-21.3	28.8	0.997
<b>3</b> (POPh <sub>2</sub> )-OMs (trans)	27.5	13.35	26.8	0.3	26.7	0.9998
<b>1</b> (PSPPh <sub>2</sub> )-OMs (biased trans)	22.0	12.96	21.4	-1.3	21.7	0.9999
<b>2</b> (PSPPh <sub>2</sub> )-OMs (cis)	32.7	14.33	32.0	4.7	30.6	0.998
<b>3</b> (PSPPh <sub>2</sub> )-OMs (trans)	26.6	14.15	26.0	4.0	24.8	0.9994
cyclohexyl mesylate <sup>a</sup>	18.0	7.72	17.3	-25.5	24.9	

<sup>a</sup> Parameters calculated from ref 5. <sup>b</sup> Correlation coefficient.

**Table 4.** Product Studies (%)

substrate	product	97% TFE	80% EtOH
<b>1</b> (POPh <sub>2</sub> )-OMs (biased trans)	<b>4</b> (R = <i>t</i> -Bu)	81	80
	<b>5</b> (R = <i>t</i> -Bu)	11	9
	<b>6</b> (X = OEt)		6
	<b>6</b> (X = OCH <sub>2</sub> CF <sub>3</sub> )	4	
<b>2</b> (POPh <sub>2</sub> )-OMs (cis)	<b>6</b> (X = OH)	4	5
	<b>4</b> (R = H)	44	15
	<b>5</b> (R = H)	47	78
	<b>3</b> (POPh <sub>2</sub> ) (X = OEt)		3
	<b>3</b> (POPh <sub>2</sub> ) (X = OCH <sub>2</sub> CH <sub>3</sub> )	5	
<b>3</b> (POPh <sub>2</sub> )-OMs (trans)	<b>3</b> (POPh <sub>2</sub> ) (X = OH)	4	4
	<b>4</b> (R = H)	81	90
	<b>5</b> (R = H)	12	10
<b>1</b> (PSPPh <sub>2</sub> )-OMs (biased trans)	<b>2</b> (POPh <sub>2</sub> ) (X = OCH <sub>2</sub> CF <sub>3</sub> )	7	
	<b>7</b> (R = <i>t</i> -Bu)	100	100
<b>2</b> (PSPPh <sub>2</sub> )-OMs (cis)	<b>7</b> (R = H)	42	11
	<b>8</b>	58	89
<b>3</b> (PSPPh <sub>2</sub> )-OMs (trans)	<b>7</b> (R = H)	100	100

**Table 5.** Rate Ratios in 97% Trifluoroethanol

substrate	25 °C	70 °C
cyclohexyl	1.0 <sup>a</sup>	1.0 <sup>a</sup>
<b>1'</b> (PO(OEt) <sub>2</sub> ) (biased trans)	0.069	0.13
<b>2</b> (PO(OEt) <sub>2</sub> ) (cis)	0.0054	0.038
<b>1'</b> / <b>2</b> (PO(OEt) <sub>2</sub> )	12.7 <sup>b</sup>	3.5 <sup>b</sup>
<b>1</b> (POPh <sub>2</sub> ) (biased trans)	0.63	3.0
<b>2</b> (POPh <sub>2</sub> ) (cis)	0.0014	0.0043
<b>1'</b> / <b>2</b> (POPh <sub>2</sub> )	440	700
<b>1</b> (PSPPh <sub>2</sub> ) (biased trans)	220	520
<b>2</b> (PSPPh <sub>2</sub> ) (cis)	7.0 × 10 <sup>-5</sup>	0.0018
<b>1'</b> / <b>2</b> (PSPPh <sub>2</sub> )	3.2 × 10 <sup>6</sup>	2.9 × 10 <sup>5</sup>

<sup>a</sup> Rate ratios in this column are with respect to cyclohexyl tosylate ( $1.70 \times 10^{-6} \text{ s}^{-1}$  at 25 °C,  $2.77 \times 10^{-4} \text{ s}^{-1}$  at 70 °C) for the diethyl phosphonate and with respect to cyclohexyl mesylate ( $3.24 \times 10^{-6} \text{ s}^{-1}$  at 25 °C,  $1.79 \times 10^{-4} \text{ s}^{-1}$  at 70 °C) for the oxide and sulfide. <sup>b</sup> Rate ratios in this column are for the biased trans form **1** to the cis form **2** for each system.

which may include steric effects, induction, and the two modes of  $\beta$ -effect activity. Secondly, the ratio of the biased trans ( $\sim 180^\circ$ ) to cis ( $\sim 60^\circ$ ) forms provides a measure of stereochemically dependent components of the  $\beta$  effect. The bridge-forming nonvertical process (path A) should be possible only in the antiperiplanar ( $180^\circ$ ) stereochemistry. Hyperconjugation (path B) should have a cosine-squared dependence, with maxima at  $0^\circ$  and  $180^\circ$  and a minimum at  $90^\circ$ . The  $\beta$  effect thus should be vastly reduced in the cis stereochemistry by either mechanism. If only an inductive effect is operating, the cis and biased trans forms should have about the same rate.

Table 5 contains these rate comparisons for the phosphonate,<sup>9</sup> oxide, and sulfide (it should be noted from Scheme 2 that in

the biased trans phosphonate **1'** the *tert*-butyl group is at a different location from **1** for the oxide and sulfide, but the change has no bearing on these comparisons). The cis forms should provide a measure of the polar effect of the  $\beta$  substituent. At 25 °C, the cis phosphonate solvolyzes about 180 times more slowly than cyclohexyl in 97% TFE, the cis oxide 700 times more slowly, and the cis sulfide 20 000 times more slowly. These results indicate that the phosphine sulfide is the most electron-withdrawing group. The polar effects are discussed more extensively in the section on calculational results. In each case, however, the slow rates of the cis forms document polar inhibition of the solvolysis process for the synclinal stereochemistry. The mechanism probably involves rate-determining reaction with solvent.

Again at 25 °C, the biased trans phosphonate solvolyzes only 14 times more slowly than cyclohexyl. We characterized this reduced ratio as the result of a weak but significant  $\beta$  effect of diethyl phosphonate.<sup>9</sup> The biased trans phosphine oxide is only 1.5 times as slow as cyclohexyl, and in the more ionizing solvent HFIP (Table 1) the oxide is 3.4 times faster than cyclohexyl. Thus the  $\beta$  effect of diphenylphosphine oxide is just sufficient to overcome the strong polar effect of the group. Finally, the sulfide clearly qualifies as a strong  $\beta$ -effect group, as the biased trans form reacts 220 times faster than cyclohexyl.

In terms of the biased trans to cis ratios, the figures for the phosphonate, oxide, and sulfide respectively are 12.8, 450, and  $3.2 \times 10^6$ . Table 5 also shows the values for these ratios at 70 °C, for which the trends are the same. Thus kinetic extrapolations do not influence the interpretations. These results show that the phosphine sulfide is a very strong  $\beta$ -effect group despite its large polar effect, the phosphine oxide is respectable, and the previously studied phosphonate is weak.

**Molecularity.** We have used the method developed by Raber, Harris, and their co-workers for the assessment of molecularity under these pseudo-first-order conditions.<sup>13</sup> These authors constructed plots of reaction rates in aqueous ethanol and aqueous TFE, with the substrate on the *y* coordinate and 1-adamantyl bromide on the *x* coordinate. A substrate reacting by an ionization mechanism (either carbocation ( $k_c$ ) or anchimeric assistance ( $k_A$ )) gives a single straight line, since the rates on both coordinates are responding to the same factors. Increased water content in aqueous ethanol enhances solvent ionizing power but has little effect on nucleophilicity. In contrast, increased water content in aqueous TFE enhances solvent nucleophilicity but has little effect on ionizing power. Raber and Harris found that reactions in which solvent is present

(13) Raber, D. J.; Neal, W. C., Jr.; Dukes, M. D.; Harris, J. M.; Mount, D. L. *J. Am. Chem. Soc.* **1978**, *100*, 8137–8146. Harris, J. M.; Mount, D. L.; Smith, M. R.; Neal, W. C., Jr.; Dukes, M. D.; Raber, D. J. *J. Am. Chem. Soc.* **1978**, *100*, 8147–8156.

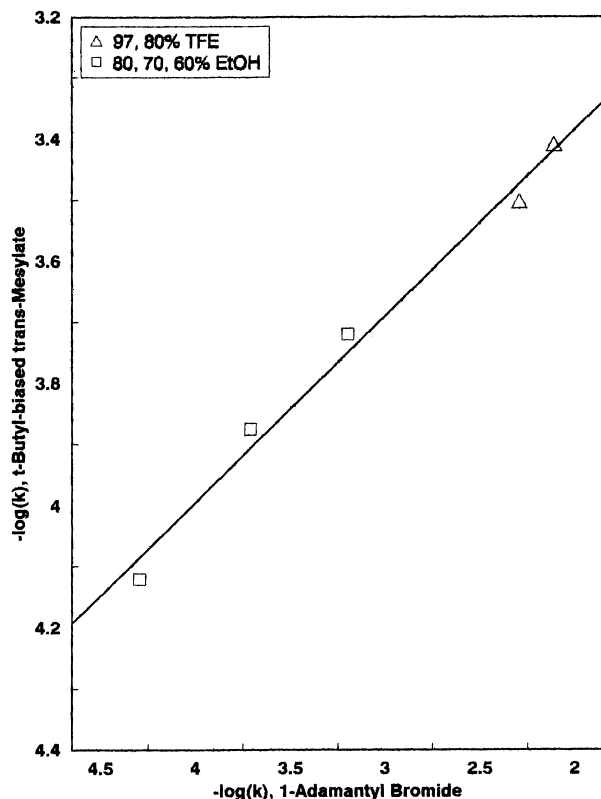


**Figure 1.** Raber-Harris plot for *r*-4-*tert*-butyl-*trans*-2-(diphenylphosphinoyl)cyclohex-*cis*-1-yl mesylate (**1**(P(O)Ph<sub>2</sub>)-OMs).

in the transition state ( $S_N2$  or  $E_2$ , also called  $k_s$ ) generally give two separate, diverging lines for the two solvents. The slope for the TFE points is greater than that for ethanol because the rates in TFE are changing faster for the  $y$  than the  $x$  axis.

In the case of the diethyl phosphonate,<sup>9</sup> we found that the *cis* substrate **2**(PO(OEt)<sub>2</sub>) produced a two-line plot that is typical of a bimolecular ( $k_s$ ) process, but the biased *trans* substrate **1'**(PO(OEt)<sub>2</sub>) produced a one-line plot that is typical of an ionization process ( $k_c$  or  $k_\Delta$ ). Interestingly, the unbiased *trans* substrate **3**(PO(OEt)<sub>2</sub>) produced an intermediate plot, in which there were two lines but with little difference in slope. The appearance of this plot suggested that the mechanism was  $k_c$  or  $k_\Delta$  in the more ionizing TFE solvents but a mixture of bi- and unimolecular processes in ethanol. In ethanol some of the diequatorial form must be contributing to the rate expression with some  $k_s$  contribution.

The situation with the phosphine oxide is similar to that with the phosphonate. The biased *trans* form **1**(POPh<sub>2</sub>) produces a one-line Raber-Harris plot (Figure 1) that is clearly indicative of an ionization process ( $k_c$  or  $k_\Delta$ ). The unbiased form **3**(POPh<sub>2</sub>), like the analogous phosphonate, produces an intermediate plot (Figure 2), with the TFE points bunched in a  $k_c$  fashion but two separate lines in a  $k_s$  fashion. The correlation coefficient for all six points is 0.82, the same as for the phosphonate.<sup>9</sup> We were not able to construct a Raber-Harris plot for the *cis* substrate **2**(POPh<sub>2</sub>) because the rates were too slow to be measured in ethanol below its boiling point.

For the phosphine sulfide, the unbiased *trans* form **3**(PSPH<sub>2</sub>) produces a one-line Raber-Harris plot (Figure 3, correlation coefficient of 0.95). Even in ethanol this substrate appears to be reacting by an ionization process ( $k_c$  or  $k_\Delta$ ). As with the oxide, we were not able to construct a Raber-Harris plot for the *cis* substrate because of the exceedingly slow rates in ethanol.

The Raber-Harris test of molecularity is in consonance with the kinetic comparisons. The faster rate of the biased *trans* form, in comparison with both cyclohexyl and the *cis* form, accom-

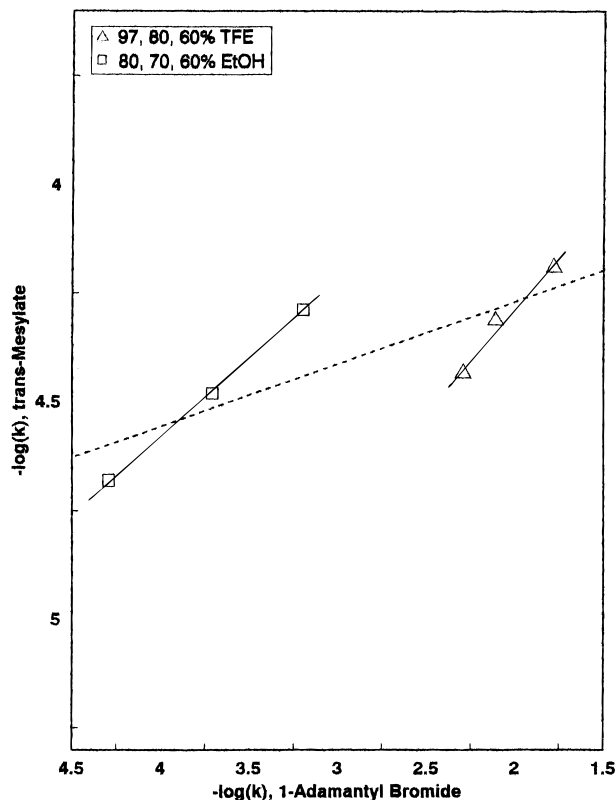


**Figure 2.** Raber-Harris plot for *trans*-2-(diphenylphosphinoyl)cyclohexyl mesylate (**3**(P(O)Ph<sub>2</sub>)-OMs).

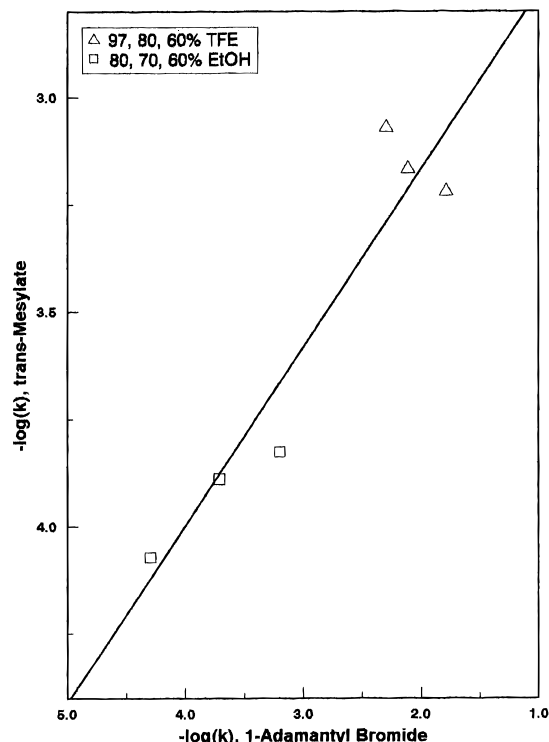


**Figure 3.** Raber-Harris plot for *trans*-2-(diphenylthiophosphinoyl)cyclohexyl mesylate (**3**(P(S)Ph<sub>2</sub>)-OMs).

panies a change in molecularity from a solvent-assisted mechanism ( $k_s$ ) to a unimolecular ionization mechanism ( $k_c$  or  $k_\Delta$ ).

**Products.** Several pertinent comments may be made concerning the product structures listed in Table 4. Firstly, the products from the *cis* oxide are consistent with a solvent-assisted reaction. Over 90% of the products result from elimination of one of the antiperiplanar protons (positions 2 and 6 with respect to the leaving group). The small amount of substitution occurs

with inversion. Secondly, the products from the trans oxide substrates require a carbocation mechanism. There is only one antiperiplanar proton, but a significant amount of the products come from elimination of a formally syn proton to give **5**. The only mechanistically viable route that avoids a syn elimination is through a carbocation intermediate that can lead to either **4** or **5**. Alternatively, phosphine oxide must be considered to favor syn elimination by an unspecified steric effect. Thirdly, the substitution products of the trans oxide substrates are formed with inversion. Such a stereochemistry is common for reaction within an ion pair. In the rate-determining step, the C–X bond is broken to form an ion pair, which shields the front side of the broken bond. Reaction of the carbocation then takes place preferentially with inversion. This last observation is pertinent to the question of vertical vs nonvertical pathways. The nonvertical pathway leads to the bridged intermediate (path A in Scheme 1) ( $M = -PPh_2-O-$ ). Solvent would react with the ring in a second inversion to form the substitution product with retention. Retained stereochemistry has been a hallmark of neighboring group participation. Thus the products do not support a nonvertical mechanism, although substitution represents <10% of the product, and need not be a definitive indicator of the major mechanism. Fourthly, the sulfides react exclusively to form elimination products. The cis sulfide gives both regiochemistries (**7** and **8**), but the trans sulfides give exclusively **7**. Strong stabilization of the carbocation by the axial phosphine sulfide group may inhibit elimination of any but the 6-axial proton. Fifthly, neither the oxide nor the sulfide yielded any fragmentation product, in which both the nucleofuge (OMs) and the electrofuge (POPH<sub>2</sub> or P(S)Ph<sub>2</sub>) are eliminated to form a hydrocarbon. Such a product might be expected when the electrofuge bears an appreciable positive charge through hyperconjugation. Hagen and Mayr,<sup>14</sup> however, obtained similar results in elimination reactions involving the X–C–C–Si bonds. They found that the amount of desilylation decreased when the silicon atom bore bulky substituents. Attack of the nucleophilic species then was directed more to carbon than to silicon. The bulky phenyl rings may fulfill a similar role in the present cases.

Product analysis thus is a mixed bag. The presence of inverted rather than retained substitution products is consistent with a vertical rather than a nonvertical mechanism, but these products are observed only for the oxide and then in <10%. The elimination products are consistent with a carbocation process in the case of the trans substrates.

**Isotope Effects.**  $\alpha$ -Secondary deuterium kinetic isotope effects have been used widely in solvolysis reactions as a probe for the hybridization of the carbon atom bearing the nucleofuge.<sup>15</sup> In a carbocation-forming reaction such as the vertical ( $k_c$ ) process (path B in Scheme 1), the carbon atom changes from sp<sup>3</sup> in the ground state to sp<sup>2</sup> in the intermediate, with a transition state moving toward sp<sup>2</sup>. The  $\alpha$ -hydrogen deuterium isotope effect is normally in the range 1.15–1.25 for such a process. For an S<sub>N</sub>2 reaction, with either direct displacement by the solvent ( $k_s$ ) or internal displacement of the nucleofuge by the electrofuge to form a ring (path A,  $k_A$ ), the  $\alpha$ -isotope effect is small or even inverse (0.95–1.05). We applied this method to the  $\beta$ -effect role of silicon and found an isotope effect of 1.17 in TFE at 25 °C, experimentally the same as the 1.18 for 2-adamantyl tosylate, in which the process clearly is carbocation formation, under the same conditions.<sup>6</sup>

## Chart 1

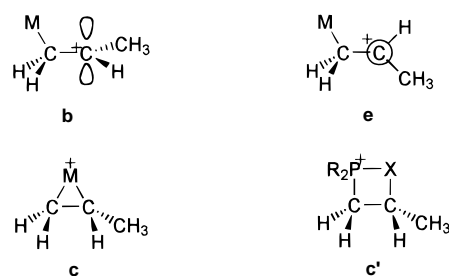


**Table 6.** Hyperconjugative Ability as Measured by the Energy Difference Between the Parallel (b) and Perpendicular (e) Forms ( $\Delta E_{be}$ , kcal mol<sup>-1</sup>) of M–CH<sub>2</sub>–C<sup>+</sup>HCH<sub>3</sub>

M	RHF/6-31G(d)	MP2/6-31G(d)
PH <sub>2</sub>	14.35	22.94
P(O)H <sub>2</sub>	4.72	8.80
P(S)H <sub>2</sub>	3.93	10.54
P(O)(OH) <sub>2</sub>	4.27	7.98
SiH <sub>3</sub> <sup>a</sup>	16.02	22.20

<sup>a</sup> Data from ref 18.

We observed a  $k_H/k_D$  of  $1.21 \pm 0.01$  for the phosphine oxide at 55.0 °C and  $1.26 \pm 0.04$  for the phosphine sulfide at 35.1 °C in 97% TFE. These figures are strong evidence for a transition state with high sp<sup>2</sup> character, as expected for the vertical and not the nonvertical process. Formation of a five-membered ring in the  $k_A$  reaction of MeO(CH<sub>2</sub>)<sub>3</sub>CHMeOBs exhibited a reduced  $k_H/k_D$  of 1.08.<sup>16</sup> To the extent that these secondary isotope effects are valid indicators of transition state structure, these observations are consistent with an open carbocation (path B) rather than a bridged structure (path A).

## Calculational Results and Discussion

The calculational work of Jorgensen and his co-workers<sup>17,18</sup> provided considerable insight into the  $\beta$  effect of silicon. Consequently, we have carried out analogous calculations on the effects of four phosphorus groups ( $M = PH_2$ , P(=O)H<sub>2</sub>, P(=S)H<sub>2</sub>, and P(=O)(OH)<sub>2</sub>). In addition to the hydrogen-substituted analogues of the present and previous<sup>9</sup> study, we include the phosphine group, which has not been studied experimentally because of its high reactivity with air and water. As a measure of the hyperconjugative  $\beta$  effect, we compared the energies of two conformations, in which the P–C bond is either parallel to the empty orbital (the form Jorgensen called bisected or b)<sup>17,18</sup> or perpendicular (Jorgensen's eclipsed form or e), as seen in Chart 1. Hyperconjugation is optimal in the parallel or b form and minimal in the perpendicular or e form. In addition, we calculated the energies of the bridged form (called cyclic or c by Jorgensen), which is a three-membered ring for the phosphine (c in Chart 1,  $M = PH_2$ ) and a four-membered ring for the oxide, sulfide, or phosphonate (c' in Chart 1: when M is P(O)(OH)<sub>2</sub>, R = OH and X = O; when M is P(O)H<sub>2</sub>, R = H and X = O; when M is P(S)H<sub>2</sub>, R = H and X = S).

Table 6 contains the difference in energy ( $\Delta E_{be}$ ) between the parallel and perpendicular forms at two levels of calculation for the four phosphorus functional groups as well as Jorgensen's calculations for the silicon group<sup>18</sup> ( $M = SiH_3$ ). The quantity  $\Delta E_{be}$  is a measure of hyperconjugation, which is maximal in the parallel (b) form and absent in the perpendicular (e) form.

(14) Hagen, G.; Mayr, H. *J. Am. Chem. Soc.* **1991**, *113*, 4954–4961.

(15) Isaacs, N. *Physical Organic Chemistry*; Longman: Essex, U.K., 1987; pp 265, 394–395, 599–600. Shiner, V. J., Jr. In *Isotope Effects in Chemical Reactions*; Collins, C. J.; Bowman, N. S., Eds.; Van Nostrand Reinhold: New York, 1970; pp 104–137. Harris, J. M. *Prog. Phys. Org. Chem.* **1974**, *11*, 103–108.

(16) Eliason, R.; Tomič, M.; Borčić, S.; Sunko, D. E. *Chem. Commun.* **1968**, 1490–1491.

(17) Wierschke, S. G.; Chandrasekhar, J.; Jorgensen, W. L. *J. Am. Chem. Soc.* **1985**, *107*, 1496–1500.

(18) Ibrahim, M. R.; Jorgensen, W. L. *J. Am. Chem. Soc.* **1989**, *111*, 819–824.

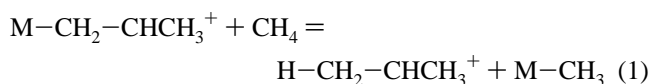
**Table 7.**  $\beta$ -Effect Stabilization ( $M-\text{CH}_2\text{C}^+\text{HCH}_3 + \text{CH}_4 = \text{H}-\text{CH}_2\text{C}^+\text{HCH}_3 + M-\text{CH}_3$ )

system <sup>c</sup>	$-E,^a$ au		$\Delta E,^b$ kcal mol <sup>-1</sup>	
	RHF/6-31G(d)	MP2/6-31G(d)	RHF/6-31G(d)	MP2/6-31G(d)
H-CH <sub>3</sub>	40.195 17	40.332 44		
H-CH <sub>2</sub> CH <sup>+</sup> CH <sub>3</sub>	117.381 16	117.745 52	0	0
PH <sub>2</sub> -CH <sub>3</sub>	381.486 26	381.720 91		
b-PH <sub>2</sub> -CH <sub>2</sub> CH <sup>+</sup> CH <sub>3</sub>	458.690 61	459.169 51	11.52	22.29
e-PH <sub>2</sub> -CH <sub>2</sub> CH <sup>+</sup> CH <sub>3</sub> <sup>d</sup>	458.667 73	459.132 95	-2.83	-0.65
c-PH <sub>2</sub> -CH <sub>2</sub> CH <sup>+</sup> CH <sub>3</sub>	458.692 41	459.182 77	12.66	30.61
P(O)H <sub>2</sub> -CH <sub>3</sub>	456.360 85	456.779 25		
b-P(O)H <sub>2</sub> -CH <sub>2</sub> CH <sup>+</sup> CH <sub>3</sub>	533.542 83	534.197 80	-2.51	3.44
e-P(O)H <sub>2</sub> -CH <sub>2</sub> CH <sup>+</sup> CH <sub>3</sub> <sup>d</sup>	533.535 32	534.183 79	-7.23	-5.36
c-P(O)H <sub>2</sub> -CH <sub>2</sub> CH <sup>+</sup> CH <sub>3</sub>	533.580 98	534.241 67	21.43	30.96
P(S)H <sub>2</sub> -CH <sub>3</sub>	779.015 84	779.369 78		
b-P(S)H <sub>2</sub> -CH <sub>2</sub> CH <sup>+</sup> CH <sub>3</sub>	856.190 51	856.788 77	-7.10	3.71
e-P(S)H <sub>2</sub> -CH <sub>2</sub> CH <sup>+</sup> CH <sub>3</sub> <sup>d</sup>	856.184 26	856.771 98	-11.03	-6.83
c-P(S)H <sub>2</sub> -CH <sub>2</sub> CH <sup>+</sup> CH <sub>3</sub>	856.237 62	856.846 98	22.46	40.24
P(O)(OH) <sub>2</sub> -CH <sub>3</sub>	606.172 36	606.947 49		
b-P(O)(OH) <sub>2</sub> -CH <sub>2</sub> CH <sup>+</sup> CH <sub>3</sub> <sup>d</sup>	683.356 73	684.368 13	-1.02	4.74
e-P(O)(OH) <sub>2</sub> -CH <sub>2</sub> CH <sup>+</sup> CH <sub>3</sub> <sup>d</sup>	683.349 92	684.355 40	-5.29	-3.24
c-P(O)(OH) <sub>2</sub> -CH <sub>2</sub> CH <sup>+</sup> CH <sub>3</sub>	683.387 56	684.407 89	18.33	29.70
b-CH <sub>3</sub> -CH <sub>2</sub> CH <sup>+</sup> CH <sub>3</sub> <sup>e</sup>	156.420 80	156.917 58	4.05	6.58
b-SiH <sub>3</sub> -CH <sub>2</sub> CH <sup>+</sup> CH <sub>3</sub> <sup>e</sup>	407.481 63	407.932 89	14.83	22.13
e-SiH <sub>3</sub> -CH <sub>2</sub> CH <sup>+</sup> CH <sub>3</sub> <sup>d,e</sup>	407.456 10	407.897 52	-1.19	-0.07
c-SiH <sub>3</sub> -CH <sub>2</sub> CH <sup>+</sup> CH <sub>3</sub> <sup>d,e</sup>	407.470 70	407.926 57	7.97	18.16

<sup>a</sup> Calculated energy for a single species. <sup>b</sup> Difference in energy between the two sides of the title equation. <sup>c</sup> The prefix b signifies the parallel form in Chart 1, e the perpendicular form, and c the bridged or cyclic form. <sup>d</sup> Not an energy minimum; calculated with a constraint. <sup>e</sup> Data from ref 18.

Geometry was fully optimized at the lower level. Energies then were calculated at the higher level for the geometries found at the lower level. The MP2 calculations show uniformly higher  $\beta$  effects, and we shall consider only these in the discussion. The same trends are present in all the lower level calculations. The phosphine  $\beta$ -hyperconjugative effect is comparable to the well-known silicon  $\beta$  effect (22–23 kcal mol<sup>-1</sup>), yet it has never been observed or discussed in the literature to our knowledge, presumably because of its difficult accessibility. The other three phosphorus functionalities show a strong but smaller  $\beta$ -hyperconjugative effect, in the general range 8–11 kcal mol<sup>-1</sup>, which translates to a rate acceleration of about 1 000 000. These calculations, like Jorgensen's second set,<sup>18</sup> are on secondary carbocations, which correspond to the experimental structures. Unfortunately, the substituents on phosphorus (phenyl or ethoxy) cannot be modeled in a reasonable amount of calculation time, so that the limitations of these calculations must be appreciated not only in terms of absence of solvent effects but also in terms of simplification of the substituents.

In order to make direct comparisons between the individual forms, thereby bringing in the bridged structures (c), we used the isodesmic eq 1:



The energy difference between the left and right sides of this equation represents the difference in the ability of hydrogen and the  $\beta$ -substituent M to stabilize the positively charged vs the neutral systems. This approach removes effects present in the neutrals, so that the energy difference ( $\Delta E$ ) is a measure of the  $\beta$  effect of M vs H for a given geometry. The results are given in Table 7, along with the absolute energies of all the species.

For the phosphine and the silane,<sup>18</sup> the perpendicular form (e) is slightly destabilized by the  $\beta$  group. For the oxide, sulfide, and phosphonate, the polar effect of the new atoms destabilizes the perpendicular form by several kcal mol<sup>-1</sup>. All four phosphorus substituents show a clear stabilizing effect when the M–C bond is parallel to the empty carbocation orbital (form

b) due to hyperconjugation. Thus hyperconjugation must compensate for the polar effect to provide a rate acceleration in comparison with the hydrogen case (which is cyclohexyl for our experimental studies). The polar effects of these substituents are well documented to be strongly electron withdrawing, as measured, for example, by  $\sigma_m$  (0.55, 0.38, and 0.29, respectively, for P(O)(OEt)<sub>2</sub>, P(O)Ph<sub>2</sub>, and P(S)Ph<sub>2</sub>) or  $\sigma_1$  (0.33, 0.26, and 0.15).<sup>19a</sup> Other measurements of  $\sigma$  values reverse this order, making P(S)Ph<sub>2</sub> the most electron withdrawing:  $\sigma_m = 0.30, 0.44, \text{ and } 0.45$ , and  $\sigma_1 = 0.21, 0.30, \text{ and } 0.40$ .<sup>19b,c</sup> The perpendicular or e forms were found not to be energy minima, so the perpendicular geometry was set via the CH<sub>3</sub>–C<sup>+</sup>–C–P dihedral angle, and then all other geometric factors were optimized at the lower calculational level. The difference between the value of  $\Delta E$  for the b and e forms is  $\Delta E_{be}$  in Table 6, e.g.,  $3.71 - (-6.83) = 10.54$  for the sulfide.

The energies of the cyclic forms (c) of all phosphorus functionalities were calculated to be lower than for the parallel open forms (b), by about 8 kcal mol<sup>-1</sup> for the phosphine, 28 kcal mol<sup>-1</sup> for the oxide, 36 kcal mol<sup>-1</sup> for the sulfide, and 25 kcal mol<sup>-1</sup> for the phosphonate. Thus the bridged forms are the global minima for all cases, although the effect of the omitted ethyl or phenyl substituents is ignored. These huge stabilizations clearly are not reflected in the kinetics. Thus the cyclic phosphonate is stabilized by 29.70 kcal mol<sup>-1</sup> compared with the H system (H–CH<sub>2</sub>CH<sup>+</sup>CH<sub>3</sub>), but the diethyl derivative solvolyzes more slowly than the H comparison (cyclohexyl tosylate). Moreover, studies of acyclic carbonyl systems showed no kinetic evidence for four-membered ring formation.<sup>8</sup> The kinetics more closely follow the hyperconjugation trends.

For each parallel conformation, the energies in Tables 6 and 7 correspond to the lowest energy form. Rotation about the P–C bond, however, can generate a family of conformations. We calculated the energy of the parallel (b) form as a function of rotation around the P–C bond at 15° intervals for the phosphine and the oxide. Figure 4 shows the results for the phosphine. As seen from the structures on the figure, the lowest

(19) (a) Hansch, C.; Leo, A. *Substituent Constants for Correlation Analysis in Chemistry and Biology*; John Wiley & Sons: New York, 1979. (b) Prikoszovich, W.; Schundlbauer, H. *Chem. Ber.* **1969**, *102*, 2922–2929. (c) Johnson, A. W.; Jones, H. L. *J. Am. Chem. Soc.* **1968**, *90*, 5232–5236.



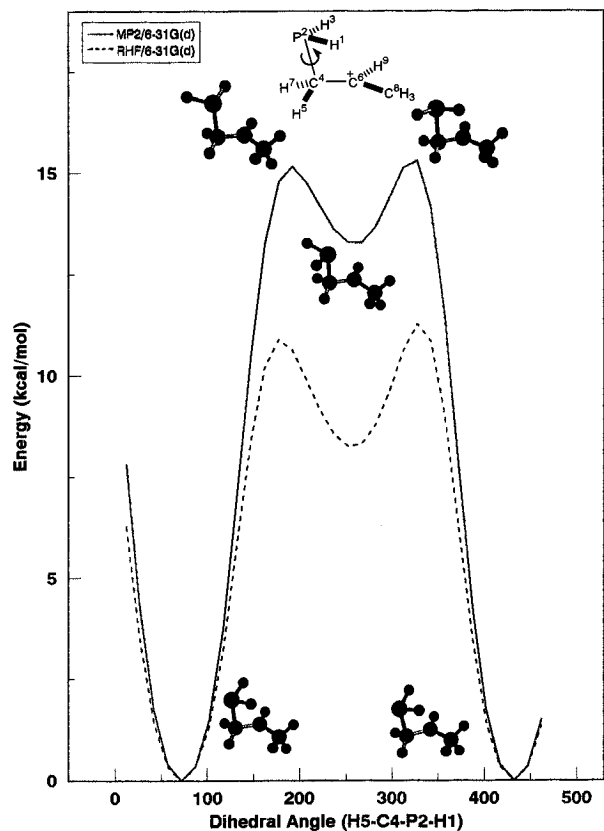
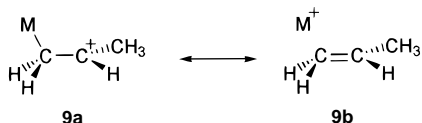


**Figure 4.** Energy of  $\text{PH}_2\text{-CH}_2\text{-CHCH}_3^+$  as a function of rotation around the P-C bond. Structures are illustrated at the dihedral angles  $72^\circ$ ,  $177^\circ$ ,  $252^\circ$ ,  $327^\circ$ , and  $432^\circ$ , which correspond to local minima or maxima.

energy form (dihedral angle of about  $180^\circ$ ) has the lone pair antiperiplanar to the C-C<sup>+</sup> bond, i.e., adverse to bridge formation. There is a higher energy minimum at about  $0^\circ$ , when the lone pair approximately eclipses the C-C<sup>+</sup> bond, favorable for bridge formation. For the oxide (Figure 5), the lowest energy form is close to  $0^\circ$ , with the P=O bond nearly eclipsed with the C-C<sup>+</sup> bond and favorable for bridging. The minimum energy angle of about  $30^\circ$  probably results in order to avoid H-H eclipsing. There is a second, higher energy minimum at about  $180^\circ$ , when the P=O bond is antiperiplanar to the C-C<sup>+</sup> bond and unfavorable for bridging.

The conformations of these carbocations therefore are determined by two major factors: (1) Polar effects influence the arrangement around the C-P bond, so that the negative end of the dipole is close to the positive charge; and (2) hyperconjugation controls the arrangement around the C-C<sup>+</sup> bond, so that the empty p orbital is parallel to the C-P bond. Eclipsing and nonbonded interactions also contribute, particularly when the bulky phenyl groups are present.

As is the case for the silane substituent,<sup>17,18</sup> hyperconjugation influences the bond lengths and angles of the phosphorus carbocations (Table 8). The valence bond structure for hyperconjugation in the parallel form (b) is depicted by **9b**, in which



the C-M bond is lengthened, the C-C<sup>+</sup> bond is shortened, and the M-C-C<sup>+</sup> angle is diminished in comparison with the perpendicular form (e), in which hyperconjugation is absent. The elongation of the C-P bond in the b form over the e form ranges from  $0.039 \text{ \AA}$  for the phosphonate to  $0.078 \text{ \AA}$  for the

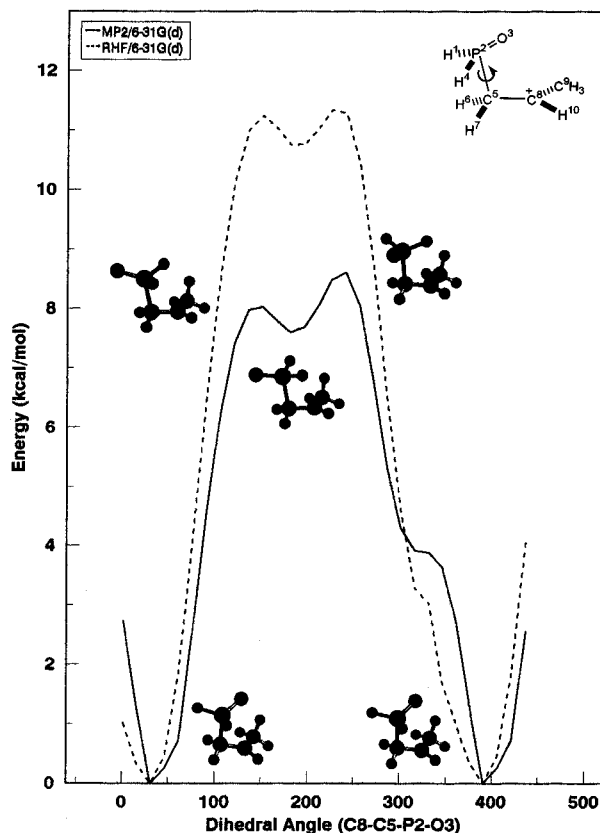


**Figure 5.** Energy of  $\text{H}_2\text{P(=O)-CH}_2\text{-CHCH}_3^+$  as a function of rotation around the P-C bond. Structures are illustrated at the dihedral angles  $38^\circ$ ,  $158^\circ$ ,  $188^\circ$ ,  $248^\circ$ , and  $398^\circ$ , which correspond to local minima or maxima.

sulfide and  $0.080 \text{ \AA}$  for the phosphine, compared with  $0.132 \text{ \AA}$  for the C-Si bond in the silane.<sup>18</sup> The diminution of the C-C<sup>+</sup> bond ranges from  $0.018 \text{ \AA}$  for the phosphonate to  $0.052 \text{ \AA}$  for the phosphine, compared with  $0.075 \text{ \AA}$  for the silane.<sup>18</sup> As the M group leans toward the carbocation, the M-C-C<sup>+</sup> angle is diminished by  $5.7^\circ$  for the oxide up to  $22.6^\circ$  for the phosphine, compared with  $19.1^\circ$  for the silane.<sup>18</sup> Thus in all cases hyperconjugation is clearly manifested by geometric distortions in the parallel form (b) that are absent in the perpendicular form (e).

### Concluding Remarks

The experimental results indicate that phosphine oxide is a modest  $\beta$ -effect group and phosphine sulfide is a strong  $\beta$ -effect group. This conclusion is supported by anti/gauche rate ratios provided by the biased trans and cis substrates **1** and **2** in 97% TFE. For the oxide the ratio is 440 at  $25^\circ\text{C}$ , and for the sulfide it is  $3.2 \times 10^6$ . Compared with cyclohexyl, the biased trans oxide reacts 0.63 times as fast and the biased trans sulfide 220 times faster. Both functionalities have compensated for a strong rate-retarding polar effect ( $\sigma_m = 0.44$  for diphenylphosphine oxide and  $0.45$  for diphenylphosphine sulfide<sup>19b</sup>). These rate ratios indicate that the electronic effects responsible for the  $\beta$  effect are extremely strong in the antiperiplanar stereochemistry for the sulfide and modest for the oxide.

One explanation for these observations that may be eliminated is polar destabilization of the ground state. Such a rationale has been put forward to explain rate accelerations for electron-withdrawing  $\alpha$ -effect groups.<sup>20</sup> When one carbon carries both the nucleofuge X and the perturbing group M (M-C-X), leading to a carbocation M-C<sup>+</sup>, the influence of M is referred

(20) Wu, Y.-D.; Kirmse, W.; Houk, K. N. *J. Am. Chem. Soc.* **1990**, *112*, 4557-4559.

**Table 8.** Geometric Comparison of the Parallel (b) and Perpendicular (e) Forms (M–C<sup>1</sup>H<sub>2</sub>–C<sup>2</sup>H<sup>+</sup>CH<sub>3</sub>)

M	P–C1 (Å)			C1–C2 (Å)			P–C1–C2 (deg)		
	b	e	b – e	b	e	b – e	b	e	b – e
PH <sub>2</sub>	1.971	1.891	0.080	1.405	1.457	–0.052	93.7	116.3	–22.6
P(O)H <sub>2</sub>	1.917	1.866	0.051	1.444	1.469	–0.025	105.1	110.8	–5.7
P(S)H <sub>2</sub>	1.951	1.873	0.078	1.435	1.464	–0.029	109.3	115.1	–5.8
P(O)(OH) <sub>2</sub>	1.873	1.834	0.039	1.447	1.465	–0.018	105.1	112.6	–7.5
SiH <sub>3</sub> <sup>a</sup>	2.070 <sup>b</sup>	1.938 <sup>b</sup>	0.132 <sup>b</sup>	1.386	1.461	–0.075	100.0 <sup>c</sup>	119.1 <sup>c</sup>	–19.1 <sup>c</sup>

<sup>a</sup> Data from ref 18. <sup>b</sup> Si–C1 bond. <sup>c</sup> Si–C1–C2 angle.

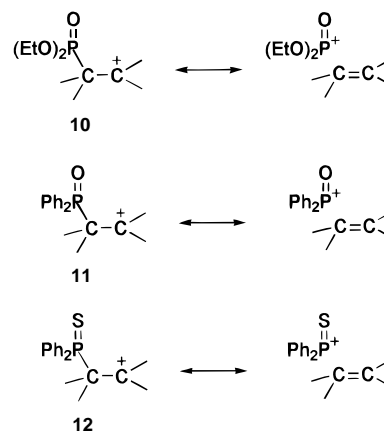
to as an  $\alpha$  effect. Rate accelerations (or smaller than expected decelerations) have been interpreted in terms of transition state stabilization through resonance delocalization,  $^+M=C<$ .<sup>21</sup> Wu et al.<sup>20</sup> pointed out that the rate changes also can be interpreted in terms of ground state destabilization, since the repulsive geminal interaction between M and X in the ground state is eliminated on loss of X. In the case of the  $\beta$ -effect accelerations in the present study, this argument is reversed. In the anti-periplanar arrangement, the C–M and C–X dipoles are *favorably* arranged, so that loss of X would cause a deceleration if anything. The observed accelerations do not support ground state repulsion effects.

Thus the positive  $\beta$  effects of phosphine oxide and sulfide must result from transition state-stabilizing effects such as those depicted in Scheme 1. The strongest case for bridging (path A) comes from the calculations. The figures in Table 7 indicate that the three- and four-membered ring intermediates (c and c' in Chart 1) represent the global energy minimum for all four cases studied (phosphine and phosphonate as well as phosphine oxide and sulfide). The effects of substituent introduction (phenyl or ethyl) might dilute this preference.

There are three lines of experimental evidence, none entirely convincing, that disfavor the bridging mechanism for the biased trans substrates (path A). (1) A bridging mechanism should produce a substitution product with retention via two inversions. The substitution products observed for the oxide (Table 4) show inverted stereochemistry, which is more in line with an ion pair carbocation mechanism. Other products from the biased trans form require the intermediacy of a carbocation to avoid a syn elimination. (2) The  $\alpha$ -hydrogen deuterium secondary isotope effects of 1.21 for the oxide and 1.26 for the sulfide support a transition state with carbocation character (path B) rather than the internal displacement transition state expected for anchimeric assistance (path A). (3) The Raber–Harris plots (Figures 1 and 3) clearly indicate a transition state lacking solvent involvement. Such one-line plots are consistent with either a carbocation ( $k_c$ , path B) or an anchimeric assistance ( $k_A$ , path A) mechanism. In their original work, Raber and Harris<sup>13</sup> offered several examples of both  $k_c$  and  $k_A$  reactions that gave one-line plots. None of their early  $k_A$  reactions, however, involved a heteroatom displacement as in Path A. Instead they were assistance by  $\sigma$  or  $\pi$  bonds. The only example of a Raber–Harris plot for a  $k_A$  reaction with a heteroatom is for systems of the type RSCH<sub>2</sub>–CH<sub>2</sub>Cl, which would form a three-membered episulfonium ion by path A.<sup>22</sup> The authors observed, however, that the reaction gave a two-line plot, seemingly indicative of solvent assistance. They eventually interpreted the results not in terms of nucleophilic solvent assistance for removal of the leaving group but instead in terms of electrophilic solvent assistance.<sup>23</sup> In contrast,

the Raber–Harris plots for the biased trans oxide and the trans sulfide are one line, so they do not resemble the example of sulfur participation.

The calculations summarized in Tables 6–8 clearly demonstrate that all these phosphorus functionalities can provide hyperconjugative stabilization for a  $\beta$  carbocation, in terms of both energetics and structural perturbations. The effect of phosphine is as strong as the well-studied effect of silane. More surprising is that the strongly electron-withdrawing groups can provide hyperconjugation valued at 8–11 kcal mol<sup>–1</sup> at the MP2 level (Table 6). The hyperconjugated valence structures **9b** would have the structures **10–12** respectively for the diethyl



phosphonate, the diphenylphosphine oxide, and the diphenylphosphine sulfide. Table 7 shows that, at the MP2 level, inductive destabilization is about 3–6 kcal mol<sup>–1</sup> (values for the perpendicular or e form) but that stabilization in the parallel or b form is more than enough to make up for this problem. Thus hyperconjugation of phosphonate, phosphine oxide, and phosphine sulfide is a calculational reality.

Whether hyperconjugation of these groups is an experimental reality is less clear. Although there is some evidence against the bridging pathway, there is no evidence that is compelling for the vertical pathway, the secondary isotope effect being its strongest argument. These interesting phosphorus functionalities thus require further examination.

## Experimental Section

### *trans*-2-(Diphenylphosphinoyl)cyclohexanol (3(P(O)Ph<sub>2</sub>)-OH).<sup>24</sup>

An oven-dried, N<sub>2</sub>-flushed, 400 mL, round-bottomed flask was equipped with a Claisen adapter to which a rubber septum and a condenser had been fitted. The vessel was charged with a magnetic stirring bar, Li (1.12 g, 0.16 mol), PPh<sub>3</sub> (21.12 g, 0.08 mol), and 160 mL of anhydrous tetrahydrofuran (THF). During 1 h of stirring, an exothermic reaction took place and the color turned deep red and then intensified to black. *tert*-Butyl chloride (7.46 g, 0.08 mol) in dry THF (20 mL) was introduced slowly into the solution via a syringe. The reaction mass was stirred for another 15 min before it was heated to reflux for 30

(21) Gassman, P. G.; Talley, J. J. *J. Am. Chem. Soc.* **1980**, *102*, 1214–1216.

(22) McManus, S. P.; Neamati-Mazraeh, N.; Hovanes, B. A.; Paley, M. S.; Harris, J. M. *J. Am. Chem. Soc.* **1985**, *107*, 3393–3395.

(23) Harris, J. M.; McManus, S. P.; Sedaghat-Herati, M. R.; Neamati-Mazraeh, N.; Kamlet, M. J.; Doherty, R. M.; Taft, R. W.; Abraham, M. H. In *Nucleophilicity*; Harris, J. M., McManus, S. P., Eds.; American Chemical Society: Washington, DC, 1987; pp 247–254.

(24) Bridges, A. J.; Whitham, G. H. *J. Chem. Soc., Chem. Commun.* **1974**, 142–143. Aguilar, A. M.; Beisler, J.; Mills, A. *J. Org. Chem.* **1962**, *27*, 1001–1011.

min. The mixture was cooled to 0 °C with an ice bath, and cyclohexene oxide (4.05 g, 0.04 mol) in THF (20 mL) was added dropwise to the solution through a syringe. The solution was allowed to warm to room temperature and stirred overnight. Addition of 5% acetic acid (20 mL) changed the color of the solution to pale green. Then 10% H<sub>2</sub>O<sub>2</sub> (60 mL) was introduced slowly into the system with cooling by an ice bath. The solution was stirred at 0 °C for another 4 h and extracted with CHCl<sub>3</sub> (3 × 50 mL). The combined organic solution was dried (MgSO<sub>4</sub>) and concentrated, and the residue was crystallized from acetone–petroleum ether to yield 9.80 g (79%) of a white solid: mp 150–152 °C; <sup>1</sup>H NMR (CDCl<sub>3</sub>)  $\delta$  0.86–1.50 (m, 4H), 1.58–1.82 (m, 3H), 2.12 (m, 1H), 2.54 (m, 1H), 5.42 (s, 1H), 7.46–7.54 (m, 6H), 7.56–7.84 (m, 4H); <sup>13</sup>C NMR (CDCl<sub>3</sub>)  $\delta$  24.0, 25.5 (d,  $J_{CP}$  = 13.1 Hz), 26.6, 35.3 (d,  $J_{CP}$  = 10.2 Hz), 44.2 (d,  $J_{CP}$  = 69.2 Hz), 69.5 (d,  $J_{CP}$  = 5.4 Hz), 128.3, 128.4, 128.7, 128.9, 131.0, 131.1, 132.1, 132.2, 132.4, 132.5; <sup>31</sup>P NMR (CDCl<sub>3</sub>)  $\delta$  42.0; MS (EI)  $m/z$  301 (3), 300 (M<sup>+</sup>, 11), 278 (11), 277 (27), 273 (12), 272 (61), 271 (10), 257 (29), 230 (24), 229 (100), 215 (12), 203 (20), 202 (100), 201 (57); HRMS (M<sup>+</sup>) calcd 300.1279, obsd 300.1275. Anal. Calcd for C<sub>18</sub>H<sub>21</sub>PO<sub>2</sub>: C, 71.99; H, 7.05. Found: C, 71.24; H, 6.83.

**cis-2-(Diphenylphosphinoyl)cyclohexanol (2(P(O)Ph<sub>2</sub>)-OH).** A 100 mL, round-bottomed flask charged with a magnetic stirring bar and 2.35 g (7.8 mmol) of the trans alcohol 3(P(O)Ph<sub>2</sub>)-OH was pumped under vacuum for several hours to remove any moisture. The flask then was fitted with a rubber septum and an inlet needle for N<sub>2</sub>. Anhydrous THF (50 mL) was added to the flask with a syringe, and the solution was cooled to –78 °C. On dropwise addition of BuLi (2.5 M, 10 mL) through a syringe, the solution turned red instantaneously. The solution was stirred at dry ice temperature for another 30 min before the reaction was quenched with saturated aqueous NH<sub>4</sub>-Cl solution. The solution was extracted with CHCl<sub>3</sub> (3 × 25 mL). The combined organic portions were dried (MgSO<sub>4</sub>) and concentrated. The residue was chromatographed on silica gel with acetone and petroleum ether as eluents to yield the cis isomer (0.50 g, 21%; the trans isomer was not isolated): <sup>1</sup>H NMR (CDCl<sub>3</sub>)  $\delta$  1.20–1.48 (m, 4H), 1.72–1.94 (m, 3H), 1.96–2.24 (m, 2H), 4.22 (m, 1H), 4.65 (m, 1H), 7.46–7.54 (m, 6H), 7.68–7.86 (m, 4H); <sup>13</sup>C NMR (CDCl<sub>3</sub>)  $\delta$  19.18, 19.28, 27.6 (d,  $J_{CP}$  = 12.9 Hz), 32.9 (d,  $J_{CP}$  = 10.5 Hz), 40.4 (d,  $J_{CP}$  = 70.3 Hz), 64.9 (d,  $J_{CP}$  = 7.3 Hz), 128.6, 128.7, 128.8, 128.9, 130.6, 130.7, 130.8, 131.0, 131.9; <sup>31</sup>P NMR (CDCl<sub>3</sub>)  $\delta$  39.4; HRMS (M<sup>+</sup>) calcd 300.1279, obsd 300.1276. Anal. Calcd for C<sub>18</sub>H<sub>21</sub>PO<sub>2</sub>: C, 71.99; H, 7.05. Found: C, 71.81; H, 6.96.

**r-4-tert-Butyl-trans-2-(diphenylphosphinoyl)cyclohexan-cis-1-ol (1(P(O)Ph<sub>2</sub>)-OH).** A 100 mL, two-necked, round-bottomed flask, fitted with a condenser and a rubber septum, was charged with Li (0.28 g, 40 mmol), PPh<sub>3</sub> (5.31 g, 20 mmol), dry THF (40 mL), and a magnetic stirring bar. Lithium diphenylphosphide was generated as above for 3(P(O)Ph<sub>2</sub>)-OH and allowed to react with 4-tert-butylcyclohexene oxide (1.54 g, 10 mmol, mixture of trans and cis isomers). The same oxidation and workup procedures were used as for 3(P(O)Ph<sub>2</sub>)-OH. The crude product was crystallized from acetone–hexane to yield a white powder (0.93 g, 26%), mp > 240 °C. The <sup>1</sup>H, <sup>31</sup>P, and <sup>13</sup>C NMR spectra all indicated a single product; <sup>1</sup>H–<sup>13</sup>C COSY, DEPT, and DQCOSY showed the product to be the desired compound: <sup>1</sup>H NMR (CDCl<sub>3</sub>)  $\delta$  0.69 (s, 9H), 1.24–1.39 (dq, 1H), 1.52–1.63 (m, 2H), 1.68–1.78 (m, 3H), 2.22–2.35 (tt, 1H), 2.67–2.75 (m, 1H), 4.16–4.24 (m, 1H), 7.38–7.52 (m, 6H), 7.72–7.88 (m, 4H); <sup>13</sup>C NMR (CDCl<sub>3</sub>)  $\delta$  20.4, 21.7, 27.0, 31.6, 32.5, 40.2, 41.1, 42.4, 65.6 (d,  $J_{CP}$  = 5.4 Hz), 128.5, 128.6, 128.7, 128.9, 130.8, 130.9, 131.0, 131.1, 131.46, 131.51, 131.55, 131.66; <sup>31</sup>P NMR (CDCl<sub>3</sub>)  $\delta$  33.6. Anal. Calcd for C<sub>22</sub>H<sub>29</sub>PO<sub>2</sub>: C, 74.13; H, 8.20. Found: C, 73.59; H, 7.97.

**trans-2-(Diphenylphosphinoyl)cyclohexyl Mesylate (3(P(O)Ph<sub>2</sub>)-OMs).** Mesylates were prepared according to standard procedure<sup>5</sup> in 70–95% yields: <sup>1</sup>H NMR (CDCl<sub>3</sub>)  $\delta$  1.14–1.28 (m, 1H), 1.48–1.61 (m, 2H), 1.64–1.83 (m, 4H), 2.45–2.56 (m, 1H), 2.59 (s, 3H), 2.66–2.76 (m, 1H), 4.92–5.03 (m, 1H), 7.48–7.56 (m, 6H), 7.58–7.68 (m, 2H), 7.82–7.92 (m, 2H); <sup>13</sup>C NMR (CDCl<sub>3</sub>)  $\delta$  23.3, 24.4, 24.6, 24.8, 33.7, 33.8, 38.1, 39.7, 40.6, 80.6, 128.6, 128.67, 128.73, 128.8, 130.7, 130.8, 130.9, 131.6, 131.7, 131.9, 134.0; <sup>31</sup>P NMR (CDCl<sub>3</sub>)  $\delta$  33.3.

**cis-2-(Diphenylphosphinoyl)cyclohexyl Mesylate (2(P(O)Ph<sub>2</sub>)-OMs):** <sup>1</sup>H NMR (CDCl<sub>3</sub>)  $\delta$  1.23–1.38 (m, 1H), 1.48–2.04 (m, 6H), 2.34–2.53 (m, 2H), 2.93 (s, 3H), 5.22–5.28 (m, 1H), 7.42–7.56 (m, 6H), 7.73–7.82 (m, 4H); <sup>13</sup>C NMR (CDCl<sub>3</sub>)  $\delta$  19.8, 21.4, 25.3, 32.3,

38.7, 42.0, 42.9, 76.4 (d,  $J_{CP}$  = 5.9 Hz), 128.6, 128.7, 128.8, 129.0, 130.7, 130.9, 131.1, 131.2, 131.8, 132.0, 132.1; <sup>31</sup>P NMR (CDCl<sub>3</sub>)  $\delta$  31.3.

**r-4-tert-Butyl-trans-2-(diphenylphosphinoyl)cyclohex-cis-1-yl Mesylate (1(P(O)Ph<sub>2</sub>)-OMs):** <sup>1</sup>H NMR (CDCl<sub>3</sub>)  $\delta$  0.71 (s, 9H), 1.19–1.39 (dq, 1H), 1.59–1.74 (m, 3H), 1.87–1.98 (m, 2H), 2.31–2.44 (tt, 1H), 2.91 (s, 3H), 3.05–3.13 (m, 1H), 4.99–5.05 (m, 1H), 7.40–7.55 (m, 6H), 7.72–7.80 (m, 2H), 7.90–7.98 (m, 2H); <sup>13</sup>C NMR (CDCl<sub>3</sub>)  $\delta$  20.6, 21.8, 26.9, 29.8, 32.3, 38.2, 39.2, 40.1, 41.6, 78.3 (d,  $J_{CP}$  = 9.7 Hz), 128.5, 128.7, 128.8, 128.9, 130.7, 130.9, 131.0, 131.1, 131.7, 132.06, 132.11, 132.3; <sup>31</sup>P NMR (CDCl<sub>3</sub>)  $\delta$  31.9.

**r-4-tert-Butyl-trans-2-(diphenylthiophosphinoyl)cyclohexan-cis-1-ol-1-d (1(P(O)Ph<sub>2</sub>)-OH-d):** prepared from 4-tert-butylcyclohexene-2-d oxide in the same fashion as above; <sup>1</sup>H NMR (CDCl<sub>3</sub>)  $\delta$  0.68 (s, 9H), 1.25–1.40 (dq, 1H), 1.51–1.72 (m, 4H), 1.82–1.94 (m, 1H), 2.28–2.42 (dt, 1H), 3.05–3.15 (m, 1H), 7.37–7.48 (m, 6H), 7.81–7.90 (m, 2H), 7.91–8.01 (m, 2H); <sup>13</sup>C NMR (CDCl<sub>3</sub>)  $\delta$  20.2, 22.4, 27.0, 30.8, 32.5, 39.9, 40.7 (d,  $J_{CP}$  = 22.4 Hz), 65.5 (t,  $J_{CP}$  = 19.9 Hz), 128.25, 128.34, 128.4, 128.5, 128.7, 131.1, 131.2, 131.3, 131.4, 131.6, 132.1, 133.1; <sup>31</sup>P NMR (CDCl<sub>3</sub>)  $\delta$  45.7.

**trans-2-(Diphenylthiophosphinoyl)cyclohexan-1-ol (3(P(S)Ph<sub>2</sub>)-OH).** Lithium diphenylphosphide was generated and reacted with cyclohexene oxide (2.13 g, 21.7 mmol) to give the corresponding phosphine in the same fashion as in the synthesis of the trans oxide. Elemental sulfur (2 equiv) was then added, and the mixture was stirred for about 4 h at room temperature before the reaction was quenched with water. Purification by column chromatography and crystallization gave 2.54 g (37%) of a pale yellow solid: mp 176–178 °C; <sup>1</sup>H NMR (CDCl<sub>3</sub>)  $\delta$  1.08–1.80 (m, 7H), 1.97–2.08 (m, 1H), 2.65–2.97 (m, 2H), 4.03–4.17 (m, 1H), 7.37–7.48 (m, 6H), 7.75–7.84 (m, 2H), 7.94–8.03 (m, 2H); <sup>13</sup>C NMR (CDCl<sub>3</sub>)  $\delta$  24.4, 25.5, 25.7, 25.9, 34.9, 35.1, 44.7, 45.4, 70.7 (d,  $J_{CP}$  = 4.5 Hz), 128.3, 128.4, 128.5, 128.6, 131.2, 131.3, 131.8, 131.9; <sup>31</sup>P NMR (CDCl<sub>3</sub>)  $\delta$  48.1. Anal. Calcd for C<sub>18</sub>H<sub>21</sub>PSO: C, 68.33; H, 6.69. Found: C, 68.41; H, 6.43.

**cis-2-(Diphenylthiophosphinoyl)cyclohexan-1-ol (2(P(S)Ph<sub>2</sub>)-OH).** A dry 100 mL, round-bottomed flask was charged with cis-2-(diphenylphosphinoyl)cyclohexan-1-ol (0.80 g, 2.67 mmol), pyridine (1.20 mL, 14.8 mmol), trichlorosilane (0.70 mL, 6.94 mmol), anhydrous benzene (50 mL), and a magnetic stirring bar. The mixture was heated to reflux for 3 h, and sulfur (0.40 g, 12.5 mmol) was added to the mixture. The reaction mixture was stirred overnight, the reaction quenched with 2 N NaOH until the solution became clear, and the mixture extracted with ether. Column chromatography over silica gel with acetone–hexane (1/3) as eluent gave 0.15 g (18%) of a waxy solid: <sup>1</sup>H NMR (CDCl<sub>3</sub>)  $\delta$  1.22–1.68 (m, 4H), 1.76–1.93 (m, 3H), 2.09–2.28 (m, 1H), 2.56–2.67 (m, 1H), 4.10–4.16 (m, 1H), 4.42–4.48 (s, 1H), 7.42–7.54 (m, 6H), 7.82–7.98 (m, 4H); <sup>13</sup>C NMR (CDCl<sub>3</sub>)  $\delta$  19.1, 19.7, 26.0, 33.8 (d,  $J_{CP}$  = 10.4 Hz), 41.3 (d,  $J_{CP}$  = 54.5 Hz), 65.2, 128.6, 128.7, 128.77, 128.84, 129.6, 130.3, 131.1, 131.2, 131.3, 131.4, 131.7; <sup>31</sup>P NMR (CDCl<sub>3</sub>)  $\delta$  45.6. Anal. Calcd for C<sub>18</sub>H<sub>21</sub>PSO: C, 68.33; H, 6.69. Found: C, 68.42; H, 6.72.

**r-4-tert-Butyl-trans-2-(diphenylthiophosphinoyl)cyclohex-cis-yl p-Nitrobenzoate (3(P(S)Ph<sub>2</sub>)-OPNB).** A dry 100 mL, three-necked, round-bottomed flask was charged with triphenylphosphine (5.91 g, 22.5 mmol), Li (0.28 g, 40 mmol), THF (25 mL), and a magnetic stirring bar. The flask was fitted with a stopper, condenser, and rubber septum. The reaction mixture was stirred for 1 h, and tert-butyl chloride (1.89 g, 20 mmol) in THF (6 mL) was introduced slowly. The mixture was stirred for 15 min and heated to reflux for 30 min. The reaction mixture was cooled to 0 °C with an ice bath, and 4-tert-butylcyclohexene oxide (1.54 g, 10 mmol) in THF (6 mL) was added through a syringe. The reaction mixture was stirred overnight and the reaction quenched with 5% acetic acid (10 mL). Sulfur (1.22 g, 38 mmol) was added, and the solution was stirred for 3 h more. The reaction mixture was extracted with ether. The ether layer was separated, dried, and concentrated. The residue was combined with p-nitrobenzoyl chloride (2.76 g, 15.1 mmol) and pyridine (5 mL) and stirred for 1 h. The solid was filtered off and crystallized from CHCl<sub>3</sub> and CH<sub>3</sub>OH. The first batch of crystals (0.63 g, 12%) was the pure desired compound: <sup>1</sup>H NMR (CDCl<sub>3</sub>)  $\delta$  0.76 (s, 9H), 1.38–1.66 (m, 2H), 1.68–1.80 (m, 2H), 1.86–1.95 (m, 1H), 2.24–2.36 (m, 1H), 2.58–2.74 (m, 1H), 3.34–3.44 (m, 1H), 5.43–5.49 (m, 1H), 7.40–7.53 (m, 6H), 7.90–8.00 (m, 2H), 8.05–8.17 (m, 4H), 8.22–8.27 (d, 2H); <sup>13</sup>C NMR (CDCl<sub>3</sub>)  $\delta$  21.0,

23.0, 27.0, 28.0, 32.6, 37.8, 38.5, 40.3, 71.6 (d,  $J_{CP} = 8.6$  Hz), 123.5, 128.45, 128.55, 128.6, 128.7, 130.6, 131.2, 131.4, 131.5, 131.6, 132.3, 135.9, 150.4, 163.4;  $^{31}\text{P}$  NMR ( $\text{CDCl}_3$ )  $\delta$  44.8. Anal. Calcd for  $\text{C}_{29}\text{H}_{32}\text{PSNO}_4$ : C, 66.78; H, 6.18; N, 2.69. Found: C, 65.37; H, 6.12; N, 2.63.

***r*-4-*tert*-Butyl-*trans*-2-(diphenylthiophosphinoyl)cyclohexan-1-ol (1(P(S)Ph<sub>2</sub>)-OH).** A 50 mL, round-bottomed flask was charged with the benzoate (0.63 g, 1.2 mmol),  $\text{K}_2\text{CO}_3$  (0.70 g, 5.1 mmol),  $\text{H}_2\text{O}$  (1 mL), MeOH (15 mL), and a magnetic stirring bar. The mixture was heated to reflux for 3.5 h. It was then diluted with  $\text{H}_2\text{O}$  and extracted with  $\text{CHCl}_3$ . The organic layer was separated, dried ( $\text{MgSO}_4$ ), and concentrated to give 0.43 g (96%) of a white solid:  $^1\text{H}$  NMR ( $\text{CDCl}_3$ )  $\delta$  0.68 (s, 9H), 1.25–1.40 (dq, 1H), 1.51–1.72 (m, 4H), 1.82–1.94 (m, 1H), 2.31–2.45 (tt, 1H), 3.05–3.15 (m, 1H), 4.23–4.31 (m, 1H), 7.37–7.48 (m, 6H), 7.81–7.90 (m, 2H), 7.91–8.01 (m, 2H);  $^{13}\text{C}$  NMR ( $\text{CDCl}_3$ )  $\delta$  20.3, 22.5, 27.1, 31.1, 32.6, 40.1, 40.9 (d,  $J_{CP} = 14.1$  Hz), 66.2 (d,  $J_{CP} = 5.9$  Hz), 128.3, 128.5, 128.6, 128.8, 131.1, 131.3, 131.4, 131.6, 131.7, 132.1, 133.1;  $^{31}\text{P}$  NMR ( $\text{CDCl}_3$ )  $\delta$  45.8.

***cis*-2-(Diphenylthiophosphinoyl)cyclohexyl Mesylate (2(P(S)Ph<sub>2</sub>)-OMs):**  $^1\text{H}$  NMR ( $\text{CDCl}_3$ )  $\delta$  1.24–2.08 (m, 7H), 2.38–2.52 (m, 1H), 2.56–2.68 (tt, 1H), 2.83 (s, 3H), 5.41–5.47 (m, 1H), 7.42–7.54 (m, 6H), 7.71–7.80 (m, 2H), 7.89–7.97 (m, 2H);  $^{13}\text{C}$  NMR ( $\text{CDCl}_3$ )  $\delta$  19.4, 22.5, 25.9 (d,  $J_{CP} = 12.0$  Hz), 32.8 (d,  $J_{CP} = 9.7$  Hz), 38.9, 45.0 (d,  $J_{CP} = 53.3$  Hz), 76.4 (d,  $J_{CP} = 4.7$  Hz), 128.3, 128.5, 128.8, 129.0, 129.7, 131.1, 131.3, 131.8, 132.2, 132.4, 132.5;  $^{31}\text{P}$  NMR ( $\text{CDCl}_3$ )  $\delta$  45.7.

***trans*-2-(Diphenylthiophosphinoyl)cyclohexyl Mesylate (3(P(S)Ph<sub>2</sub>)-OMs):**  $^1\text{H}$  NMR ( $\text{CDCl}_3$ )  $\delta$  1.08–1.84 (m, 7H), 2.34 (s, 3H), 2.48–2.60 (m, 1H), 2.94–3.05 (m, 1H), 5.04–5.15 (m, 1H), 7.36–7.53 (m, 6H), 7.73–7.82 (m, 2H), 8.01–8.12 (m, 2H);  $^{13}\text{C}$  NMR ( $\text{CDCl}_3$ )  $\delta$  24.0, 24.8, 25.0, 25.1, 34.6 (d,  $J_{CP} = 8.6$  Hz), 38.2, 41.2 (d,  $J_{CP} = 55.4$  Hz), 81.6 (d,  $J_{CP} = 4.5$  Hz), 128.3, 128.4, 128.5, 128.7, 131.1, 131.2, 131.3, 131.4, 131.6, 132.5, 133.5;  $^{31}\text{P}$  NMR ( $\text{CDCl}_3$ )  $\delta$  48.5.

***r*-4-*tert*-Butyl-*trans*-2-(diphenylthiophosphinoyl)cyclohex-*cis*-yl Mesylate (1(P(S)Ph<sub>2</sub>)-OMs):**  $^1\text{H}$  NMR ( $\text{CDCl}_3$ )  $\delta$  0.72 (s, 9H), 1.28–1.44 (dq, 1H), 1.60–1.76 (m, 3H), 1.92–2.02 (m, 1H), 2.14–2.25 (m, 1H), 2.61–2.74 (tt, 1H), 2.87 (s, 3H), 3.46–3.56 (m, 1H), 5.03–5.08 (m, 1H), 7.44–7.55 (m, 6H), 7.89–8.02 (m, 2H), 8.08–8.16 (m, 2H);  $^{13}\text{C}$  NMR ( $\text{CDCl}_3$ )  $\delta$  20.4, 22.5, 26.9, 29.3, 32.4, 38.2, 39.0, 39.6, 40.1, 78.5 (d,  $J_{CP} = 10.7$  Hz), 128.5, 128.6, 128.8, 130.6, 131.3, 131.5, 131.6, 131.8;  $^{31}\text{P}$  NMR ( $\text{CDCl}_3$ )  $\delta$  44.3.

***r*-4-*tert*-Butyl-*trans*-2-(diphenylthiophosphinoyl)cyclohex-*cis*-1-yl-1-*d* Mesylate (1(P(S)Ph<sub>2</sub>)-OMs-*d*):**  $^1\text{H}$  NMR ( $\text{CDCl}_3$ )  $\delta$  0.71 (s, 9H), 1.27–1.42 (dq, 1H), 1.58–1.74 (m, 3H), 1.90–2.00 (m, 1H), 2.12–2.23 (m, 1H), 2.58–2.72 (dt, 1H), 2.85 (s, 3H), 3.44–3.54 (m, 1H), 7.40–7.54 (m, 6H), 7.88–7.96 (m, 2H), 8.05–8.14 (m, 2H);  $^{13}\text{C}$  NMR ( $\text{CDCl}_3$ )  $\delta$  20.3, 22.5, 26.9, 29.2, 32.4, 38.3, 38.9, 39.6, 40.1, 128.5, 128.6, 128.8, 130.6, 131.3, 131.5, 131.6, 131.7, 131.8;  $^{31}\text{P}$  NMR ( $\text{CDCl}_3$ )  $\delta$  44.2.

**Kinetic Method.** Rates in aqueous solvents were determined conductometrically with a YSI Model 32 conductance meter. The conductance cell had a 40 mL capacity and Pt electrodes. The temperature was kept constant with a Precision H8 heating bath. Usually the concentration of the substrates was ca.  $10^{-4}$  M. All linear coefficients were 1.000 with one exception of 0.999 obtained for solvolysis of the *cis* oxide in 97% TFE at 80.0 °C.

**Product Studies.** A 0.2–0.5 M solution of the substrate in 80% ethanol or 97% trifluoroethanol (0.7 mL) was prepared in a NMR tube. The tube was sealed at room temperature and put into a constant temperature bath. After at least 10 half-lives, the sample was cooled and the tube was opened. Water was added to the sample, and the solution was extracted with ether. The organic solution was dried ( $\text{MgSO}_4$ ) and concentrated under vacuum. The structures were assigned by  $^1\text{H}$  and  $^{31}\text{P}$  NMR. Quantifications were based on the  $^{31}\text{P}$  peak heights.

**Crystal Structure of *r*-4-*tert*-Butyl-*trans*-2-(diphenylthiophosphinoyl)cyclohex-*cis*-1-yl *p*-Nitrobenzoate (1(P(O)Ph<sub>2</sub>)-OPNB).** A colorless crystal of  $\text{C}_{29}\text{H}_{32}\text{PSNO}_4$  was obtained from the slow evaporation at room temperature of a solution of  $\text{CH}_3\text{OH}$  and  $\text{CHCl}_3$ . A colorless, transparent, columnar crystal with approximate dimensions of  $0.51 \times 0.20 \times 0.08$  mm was mounted on a glass fiber using oil (Paratone-N, Exxon). All measurements were made on an Enraf-Nonius CAD4

**Table 9.** Structural Parameters for 2-(Diphenylthiophosphinoyl)cyclohexyl *p*-Nitrobenzoate

biased <i>trans</i> <sup>a</sup>		<i>cis</i> <sup>b</sup>	
Bond Distances (Å)			
O1–C6	1.467(4)	O1–C18	1.475(3)
C6–C1	1.530(5)	C18–C13	1.528(4)
C1–P	1.834(4)	C13–P	1.841(3)
P–S	1.952(2)	P–S	1.965(1)
Bond Angles (deg)			
C5–C6–O1	108.8(3)	C17–C18–O1	110.0(2)
O1–C6–C1	104.3(3)	O1–C18–C13	104.8(2)
C6–C1–P	111.7(3)	C18–C13–P	111.8(2)
C2–C1–P	114.1(3)	C14–C13–P	117.2(2)
C1–P–C18	102.7(2)	C13–P–C1	110.8(1)
C1–P–C24	106.1(2)	C13–P–C7	106.6(1)
C1–P–S	116.5(1)	C13–P–S	110.67(10)
C5–C6–C1	114.4(3)	C17–C18–C13	111.8(2)
C6–C1–C2	112.0(3)	C18–C13–C14	111.0(2)
C5–C6–C1–P	88.1(4)	C17–C18–C13–P	171.0(2)
O1–C6–C1–P	153.2(2)	O1–C18–C13–P	69.8(2)
C5–C6–C1–C2	41.4(4)	C17–C18–C13–C14	56.1(3)
O1–C6–C1–C2	77.3(4)	O1–C18–C13–C14	63.0(3)

<sup>a</sup> 1(P(S)Ph<sub>2</sub>)-OPNB; see Figure 6. <sup>b</sup> 2(P(S)Ph<sub>2</sub>)-OPNB; see Figure 7.

diffractometer with graphite monochromated Mo K $\alpha$  radiation. Cell constants and an orientation matrix for data collection were obtained from a least-squares refinement using the setting angles of 25 carefully centered reflections in the range  $20.0^\circ < 2\theta < 23.8^\circ$ . The compound has a formula weight of 521.61, belonging to the primitive monoclinic space group  $P2_1/n$  (No. 14) with  $a = 9.598(5)$  Å,  $b = 20.372(4)$  Å,  $c = 13.890(3)$  Å,  $\beta = 93.76(3)^\circ$ ,  $Z = 4$ ,  $V = 2710(1)$  Å<sup>3</sup>, and a calculated density of  $1.278$  g cm<sup>-3</sup>. Diffraction intensities were collected at  $-120 \pm 1$  °C using the  $\omega - \theta$  scan technique to a maximum  $2\theta$  of  $45.9^\circ$ . Of the 5542 reflections that were collected, 3908 were unique ( $R_{\text{int}} = 0.098$ ). The linear absorption coefficient for Mo K $\alpha$  was  $2.1$  cm<sup>-1</sup>. An empirical absorption correction was applied that resulted in transmission factors of 0.95–0.98. Lorentz and polarization corrections were applied. A correction for secondary extinction was applied ( $3.1756 \times 10^{-7}$ ). The structure was solved by direct methods and expanded with Fourier techniques.<sup>25</sup> Non-hydrogen atoms were refined anisotropically. Hydrogen atoms were included in fixed positions but not refined. The final cycle of full-matrix least-squares refinement was based on 2113 observed reflections ( $I > 3.00\sigma(I)$ ) and 326 variable parameters and converged with unweighted and weighted agreement factors of  $R = 0.040$  and  $R_w = 0.036$ . The maximum and minimum peaks on the final difference Fourier map corresponded to 0.19 and  $-0.18$  e/Å<sup>3</sup>, respectively. All calculations were performed using the teXsan (Version 5.0) crystallographic software package of Molecular Structure Corp.<sup>26</sup> Additional crystallographic details are included in the Supporting Information. Important structural parameters are given in Table 9 with reference to Figure 6.

**Crystal Structure of *cis*-2-(Diphenylthiophosphinoyl)cyclohexyl *p*-Nitrobenzoate (2(P(S)Ph<sub>2</sub>)-OPNB).** A colorless crystal of  $\text{C}_{25}\text{H}_{24}\text{SPNO}_4$  was obtained from the slow evaporation at room temperature of a solution of  $\text{CH}_3\text{OH}$  and  $\text{CHCl}_3$ . A colorless, columnar crystal with approximate dimensions of  $0.46 \times 0.17 \times 0.15$  mm was mounted on a glass fiber using oil (Paratone-N, Exxon). All measurements were made on an Enraf-Nonius CAD4 diffractometer with graphite monochromated Mo K $\alpha$  radiation. Cell constants and an orientation matrix for data collection were obtained from a least-squares refinement using the setting angles of 25 carefully centered reflections in the range  $21.9^\circ < 2\theta < 23.3^\circ$ . The compound has a formula weight of 465.50, belonging to the primitive monoclinic space group  $P2_1/n$  (No. 14) with  $a = 10.081(1)$  Å,  $b = 12.830(2)$  Å,  $c = 17.657(6)$  Å,  $\beta = 94.31(2)^\circ$ ,

(25) Sheldrick, G. M. SHELX86. In *Crystallographic Computing 3*; Sheldrick, G. M., Kruger, C., Goddard, R., Eds.; Oxford University Press: Oxford, 1985; pp 175–189. Beurskens, P. T.; Admiral, G.; Beurskens, G.; Bosman, W. P.; Garcia-Granda, S.; Gould, R. O.; Smits, J. M. M.; Smykalla, C. *The DIRDIF Program System*. Technical Report of the Crystallography Library, University of Nijmegen, The Netherlands, 1992.

(26) teXsan: *Crystal Structural Analysis Package*. Molecular Structure Corp., 3200A Research Forest Dr., The Woodlands, TX 77381. 1985 and 1992.

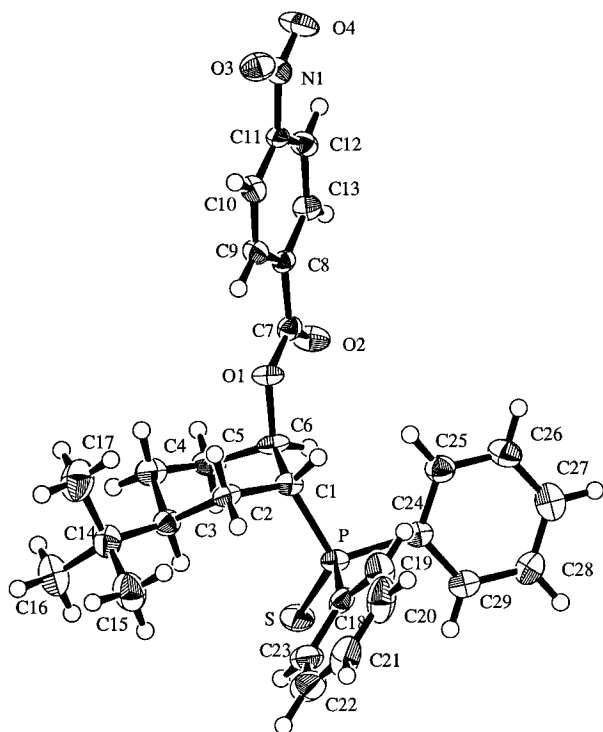


**Figure 6.** Crystal structure of *r*-4-*tert*-butyl-*trans*-2-(diphenylthiophosphinoyl)cyclohex-*cis*-1-yl *p*-nitrobenzoate (**1**(P(S)Ph<sub>2</sub>)-OPNB) with the atomic numbering system.

$Z = 4$ ,  $V = 2277.3(7) \text{ \AA}^3$ , and a calculated density of  $1.36 \text{ g cm}^{-3}$ . Diffraction intensities were collected at  $-120 \pm 1 \text{ }^\circ\text{C}$  using the  $\omega - \theta$  scan technique to a maximum  $2\theta$  of  $49.9^\circ$ . Of the 4329 reflections that were collected, 4198 were unique ( $R_{\text{int}} = 0.046$ ). The linear absorption coefficient for Mo  $K\alpha$  was  $2.4 \text{ cm}^{-1}$ . An analytical absorption correction was applied that resulted in transmission factors of 0.96–0.97. Lorentz and polarization corrections were applied. A correction for secondary extinction was applied ( $2.05192 \times 10^{-7}$ ). The structure was solved by direct methods and expanded with Fourier techniques.<sup>25</sup> Non-hydrogen atoms were refined anisotropically. Hydrogen atoms were located in the Fourier map but included in fixed positions and not refined. The final cycle of full-matrix least-squares refinement was based on 2548 observed reflections ( $I > 3.00\sigma(I)$ ) and 290 variable parameters and converged with unweighted and weighted agreement factors of  $R = 0.038$  and  $R_w = 0.033$ . The maximum and minimum peaks on the final difference Fourier map corresponded to 0.32 and  $-0.26 \text{ e/\AA}^3$ , respectively. All calculations were performed using the teXsan (Version 5.0) crystallographic software package of Molecular Structure Corp.<sup>26</sup> Additional crystallographic details are included in the Supporting Information. Important structural parameters are given in Table 9 with reference to Figure 7.

**Computational Methods.** The ab initio calculations were performed with GAUSSIAN-92<sup>27</sup> on IBM RS/6000 workstations. Full geometry optimizations were carried out by gradient methods for all neutral molecules and ions with the 6-31G(d) basis set,<sup>28</sup> which includes a set of d orbitals on all non-hydrogen atoms. The resulting geometries and basis sets were used in calculations that incorporated second-order Møller–Plesset perturbation theory to include the effects of electron correlation.<sup>29</sup> In most cases the geometry optimizations were performed

(27) Frisch, M. J.; Trucks, G. W.; Head-Gordon, M.; Gill, P. M. W.; Wong, M. W.; Foresman, J. B.; Johnson, B. G.; Schlegel, H. B.; Robb, M. A.; Replogle, E. S.; Gomperts, R.; Andres, J. L.; Raghavachari, K.; Binkley, J. S.; Gonzalez, C.; Martin, R. L.; Fox, D. J.; Defrees, D. J.; Baker, J.; Stewart, J. J. P.; Pople, J. A. *Gaussian 92*, Revision C; Gaussian Inc.: Pittsburgh, PA, 1992.

(28) Hariharan, P. C.; Pople, J. A. *Theor. Chim. Acta* **1973**, *28*, 213–222. Francl, M. M.; Pietro, W. J.; Hehre, W. J.; Binkley, J. S.; Gordon, M. S.; Defrees, D. J.; Pople, J. A. *J. Chem. Phys.* **1982**, *77*, 3654–3665.

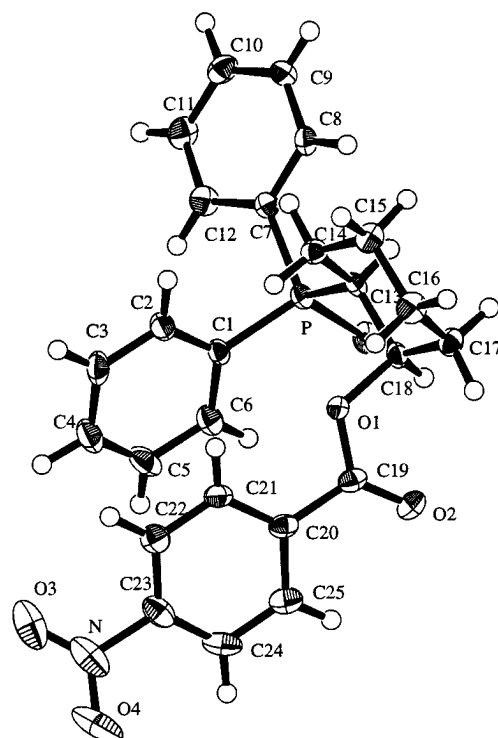


**Figure 7.** Crystal structure of *cis*-2-(diphenylthiophosphinoyl)cyclohexyl *p*-nitrobenzoate (**2**(P(S)Ph<sub>2</sub>)-OPNB) with the atomic numbering system.

with no constraints in  $C_1$  symmetry. For all carbocations, three geometric forms were considered as follows: parallel or bisected (b), perpendicular or eclipsed (e), and bridged or cyclic (c). Since the parallel forms usually are lower in energy, a constraint was made in the calculations of the perpendicular forms, in which the P–C–C–C dihedral angle was fixed at  $180^\circ$ . In the case of the  $\beta$ -phosphonate carbocation, the parallel form was not an energy minimum and closed to give the cyclic form. The parallel structure was optimized with the P–C–C bond angle fixed at  $105.1^\circ$ , which was the optimized bond angle in the  $\beta$ -phosphine oxide carbocation. For the phosphine and phosphine oxide carbocations, in order to test the effect of the rotation of the phosphorus group on  $\beta$  stabilization, the energy was calculated as the P–C bond was rotated every  $15^\circ$  with all other geometric parameters kept at the optimized values (Figures 4 and 5).

**Acknowledgment.** This work was supported by the National Science Foundation (Grant No. CHE-9302747). We thank Charlotte L. Stern for carrying out the X-ray crystal structure determinations.

**Supporting Information Available:** Listing of the crystal structure of *r*-4-*tert*-butyl-*trans*-2-(diphenylthiophosphinoyl)cyclohex-*cis*-1-yl *p*-nitrobenzoate (**1**(P(O)Ph<sub>2</sub>)-OPNB) and *cis*-2-(diphenylthiophosphinoyl)cyclohexyl *p*-nitrobenzoate (**2**(P(S)Ph<sub>2</sub>)-OPNB) (44 pages). This material is contained in many libraries on microfiche, immediately follows this article in the microfilm version of the journal, can be ordered from the ACS, and can be downloaded from the Internet; see any current masthead page for ordering information and Internet access instructions.

JA9537181

(29) Møller, C.; Plesset, M. S. *Phys. Rev.* **1934**, *46*, 618–622. Hehre, W. J.; Radom, L.; Schleyer, P. v. R.; Pople, J. A. *Ab Initio Molecular Orbital Theory*; Wiley: New York, 1986.